

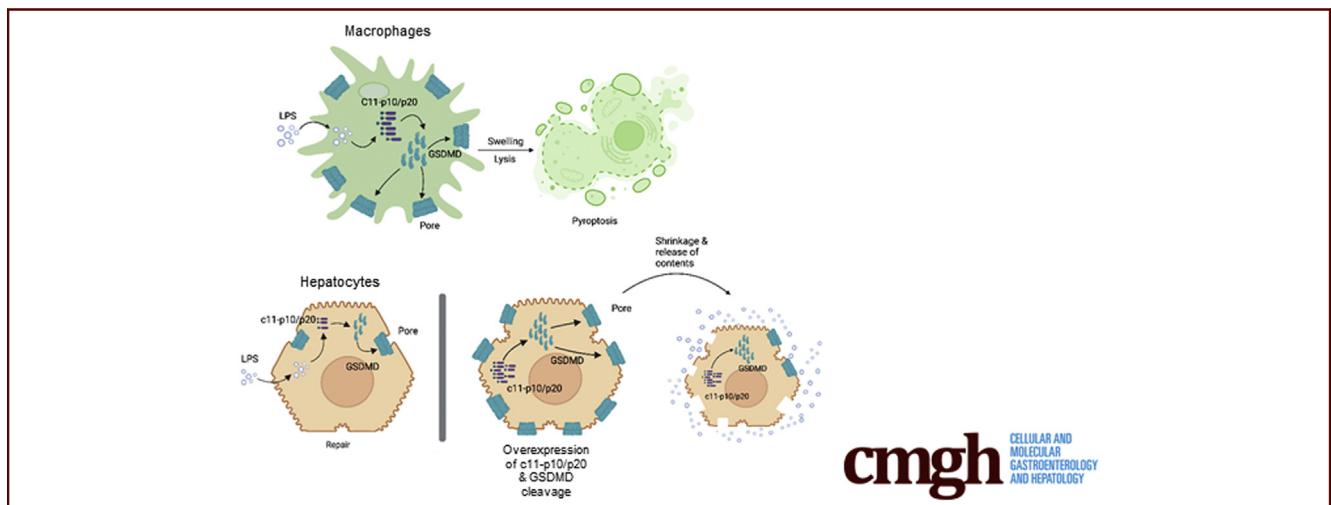
ORIGINAL RESEARCH

Hepatocytes Are Resistant to Cell Death From Canonical and Non-Canonical Inflammasome-Activated Pyroptosis



Ping Sun,^{1,2} Jie Zhong,³ Hong Liao,² Patricia Loughran,^{2,4} Joud Mulla,² Guang Fu,^{2,5} Da Tang,^{2,5} Jie Fan,^{2,6} Timothy R. Billiar,^{2,7} Wentao Gao,⁸ and Melanie J. Scott^{2,7}

¹Department of Hepatobiliary Surgery, Union Hospital, Tongji Medical College, Huazhong University of Science and Technology, Wuhan, China; ²Department of Surgery, University of Pittsburgh, Pittsburgh, Pennsylvania; ³Department of Burn and Plastic Surgery, The Second Xiangya Hospital of Central South University, Changsha, China; ⁴Center for Biologic Imaging, University of Pittsburgh, Pittsburgh, Pennsylvania; ⁵Department of General Surgery, The Third Xiangya Hospital, Central South University, Changsha, China; ⁶Research and Development, Veterans Affairs Pittsburgh Healthcare System, Pittsburgh, Pennsylvania; ⁷Pittsburgh Liver Research Center, University of Pittsburgh, Pittsburgh, Pennsylvania; and ⁸Department of Medicine, University of Pittsburgh, Pittsburgh, Pennsylvania



SUMMARY

Caspase-1/11 activation induces macrophage pyroptosis, but hepatocytes are resistant to pyroptosis, which we show is mainly due to low levels of caspase-1/11 even after stimulation. Overexpression of caspase-1/11 p10/p20 can induce hepatocyte pyroptosis and cell shrinkage, but cell structure remains relatively intact differently from macrophage pyroptosis.

BACKGROUND: Pyroptosis, gasdermin-mediated programmed cell death, is readily induced in macrophages by activation of the canonical inflammasome (caspase-1) or by intracellular lipopolysaccharide (LPS)-mediated non-canonical inflammasome (caspase-11) activation. However, whether pyroptosis is induced similarly in hepatocytes is still largely controversial but highly relevant to liver pathologies such as alcoholic/nonalcoholic liver disease, drug-induced liver injury, ischemia-

reperfusion and liver transplant injury, or organ damage secondary to sepsis.

METHODS AND RESULTS: In this study we found that hepatocytes activate and cleave gasdermin-D (GSDMD) at low levels after treatment with LPS. Overexpression of caspase-1 or caspase-11 p10/p20 activated domains was able to induce typical GSDMD-dependent pyroptosis in hepatocytes both in vitro and in vivo. However, morphologic features of pyroptosis in macrophages (eg, pyroptotic bodies, cell flattening, loss of cell structure) did not occur in pyroptotic hepatocytes, with cell structure remaining relatively intact despite the cell membrane being breached. Our results suggest that hepatocytes activate pyroptosis pathways and cleave GSDMD, but this does not result in cell rupture and confer the same pyroptotic morphologic changes as previously reported in macrophages. This is true even with caspase-1 or caspase-11 artificial overexpression way above levels seen endogenously even after priming or in pathologic conditions.

CONCLUSIONS: Our novel findings characterize hepatocyte morphology in pyroptosis and suggest alternative use for canonical/non-canonical inflammasome activation/signaling and subsequent GSDMD cleavage because there is no rapid cell death as in macrophages. Improved understanding and recognition of the role of these pathways in hepatocytes may result in novel therapeutics for a range of liver diseases. (*Cell Mol Gastroenterol Hepatol* 2022;13:739–757; <https://doi.org/10.1016/j.jcmgh.2021.11.009>)

Keywords: Liver Disease; Caspase-1; Caspase-11; Gasdermin-D; Programmed Cell Death.

The term *pyroptosis* was originally coined in 2001 to define a regulated cell death (RCD) associated with activated inflammatory caspase-1.¹ Later it was shown that inflammatory caspase-family members, including caspase-11 in mouse and caspase-4/5 in humans, also induce pyroptosis upon activation by intracellular endotoxin (lipopolysaccharide [LPS]) or Gram-negative bacteria.^{2,3} In 2015, gasdermin-D (GSDMD) was recognized as the downstream executor of pyroptosis.^{4,5} Activation of caspase-1 or caspase-11 and cleavage into their active p20 and p10 fragments enabled p20/p10 tetramer formation with the ability to cleave GSDMD directly.⁴ The N-terminus fragment of GSDMD then oligomerizes at membrane targets within the cell and at the cell membrane to form a pore in the cell that can lead to rapid proinflammatory cell death and rupture in macrophages.⁶ Other gasdermin family members have recently also been shown to be cleaved by other non-inflammatory caspases. Gasdermin-E (GSDME) can be activated by caspase-3⁷ and also by non-caspase enzymes such as neutrophil elastase⁸ and granzymes^{9,10} to induce pyroptosis.

Different from apoptosis, which is widely considered to be a non-inflammatory form of cell death, pyroptosis is considered inflammatory and is associated with release of inflammatory damage-associated molecular patterns when the cell ruptures. This inflammatory response to pyroptosis has been associated with the exacerbation of many diseases, causing organ failure and increased mortality.^{11,12} Pyroptosis has been primarily studied in macrophages, where activation of caspase-1 or -11 is essentially a death sentence. Other types of cells, including neutrophils⁸ and endothelial cells,¹³ also undergo similar rapid pyroptosis and death. However, it is less clear whether pyroptosis and cell rupture occur in hepatocytes and other epithelial cell types. Hepatocyte pyroptosis has been reported in multiple published studies investigating inflammasome activation across a range of liver diseases.^{14–17} However, there are many similar studies that have refuted the occurrence of inflammasome-mediated pyroptosis in hepatocytes under either physiological or pathologic conditions.^{13,18–21} Most of these studies occurred before the definition of pyroptosis established by the Nomenclature Committee on Cell Death in 2018, where pyroptosis is a form of RCD that critically depends on the formation of plasma membrane pores by members of the gasdermin protein family.²² Therefore, the

topic is still controversial, with little work done to define typical features of hepatocyte pyroptosis either in vitro or in vivo.


Because of our previous studies,^{18,19} we hypothesized that hepatocytes undergo pyroptosis after activation of inflammasome and GSDMD cleavage, but that they are resistant to cell rupture and classical morphologic pyroptosis under normal physiological or even pathologic circumstances. In this study we explored the mechanisms of pyroptosis using adenoviral overexpression of activated domains of caspase-1 or caspase-11, or GSDMD. Our results suggest hepatocyte pyroptosis/GSDMD cleavage can be measured and occurs at low levels because of low expression of both caspase-1 and caspase-11. Caspase-1 and -11 expression remains low even after priming or pathologic stimulation. However, morphologically hepatocytes show few changes. Hepatocyte cell death can be induced with overexpression of active fragments of caspase-1 or caspase-11, and we characterize morphologic changes for the first time in these cells. Our findings correlate with our previous findings suggesting alternative functions for canonical and non-canonical inflammasome pathways, as well as GSDMD, in hepatocytes. Understanding these pathways more fully may help us to understand pathologic mechanisms of a wide range of liver diseases and may allow us to develop novel therapeutics taking advantage of this novel signaling.

Results

Hepatocytes Are Resistant to Pyroptosis

LPS is a well-known caspase-11 activator and induces pyroptosis in macrophages.^{2,3} We treated primary hepatocytes from wild-type (WT) (C57BL/6) mice with concentrations of LPS up to 10 mg/mL for 16 hours after priming with 100 ng/mL LPS overnight and measured lactate dehydrogenase (LDH) release as a marker of lytic cell death. As a positive control for LDH release we subjected hepatocytes to a lethal concentration (5 mmol/L) of hydrogen peroxide (H₂O₂). LDH levels did not increase in LPS-treated hepatocytes compared with control (phosphate-buffered saline [PBS]-treated) hepatocytes, despite evidence of low levels of cleavage/activation of caspase-11 and cleavage of GSDMD (Figure 1A and B). We repeated the experiment but this time transfected LPS to ensure LPS entry into the cytosol. As previously, we did not see increases in LDH release despite low level cleavage/activation of caspase-11 and GSDMD in

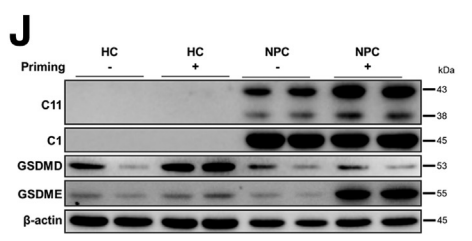
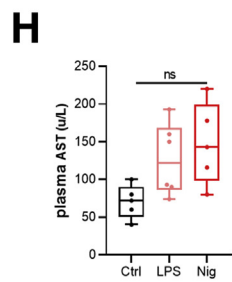
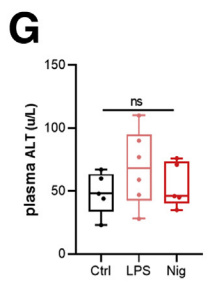
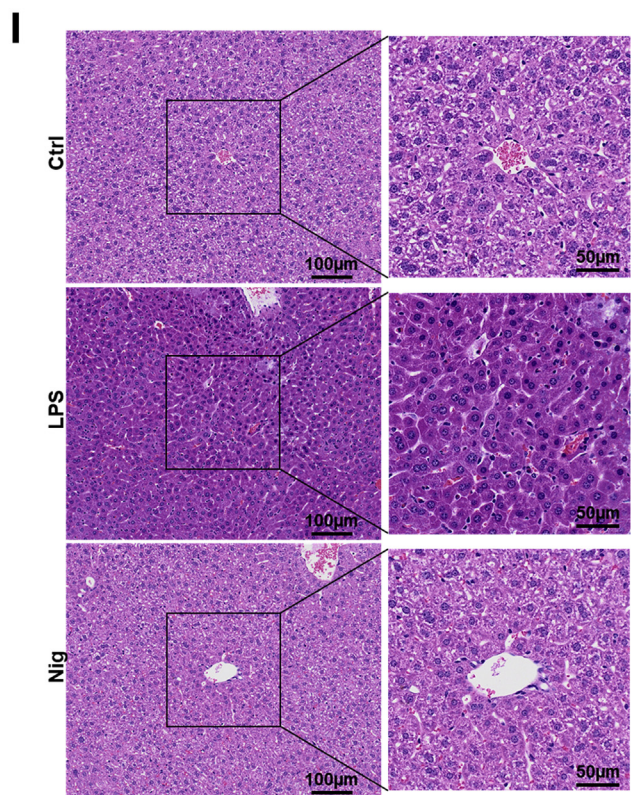
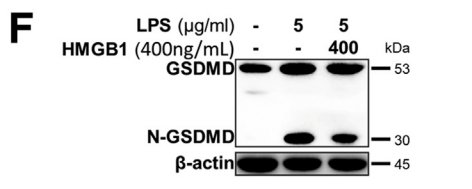
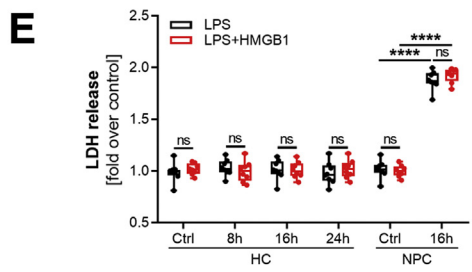
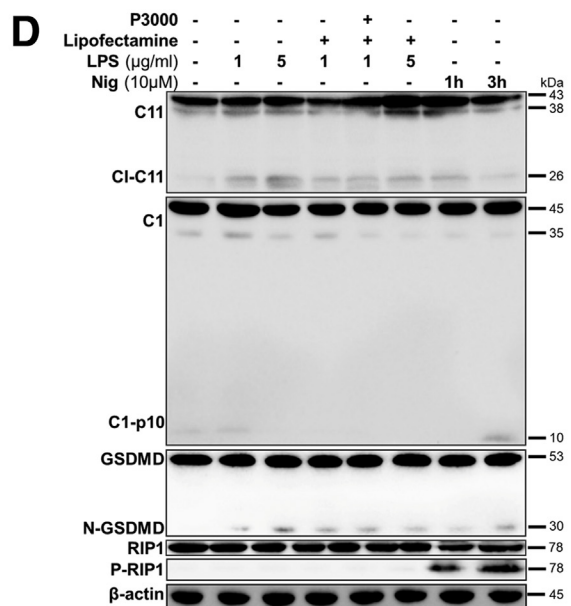
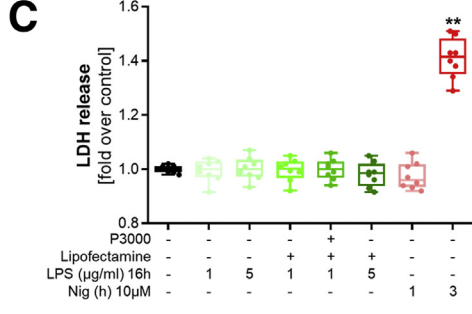
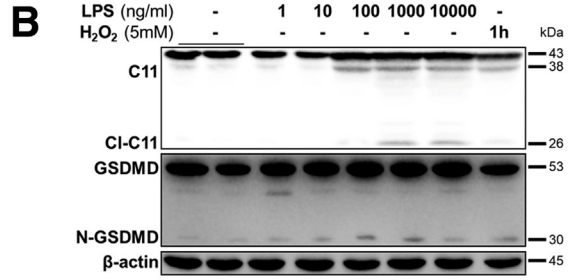
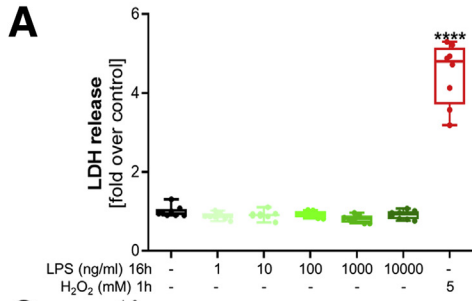
Abbreviations used in this paper: ALT, alanine aminotransferase; AST, aspartate aminotransferase; GFP, green fluorescent protein; GSDMD, gasdermin-D; GSDME, gasdermin-E; HMGB1, high mobility group box 1; IHC, immunohistochemistry; IL, interleukin; LDH, lactate dehydrogenase; LPS, lipopolysaccharide; NINJ1, nerve injury-induced protein 1; NPC, nonparenchymal cells; PBS, phosphate-buffered saline; RCD, regulated cell death; RT-PCR, real-time polymerase chain reaction; SD, standard deviation; VP, virus particles; WT, wild-type.

 Most current article

© 2021 The Authors. Published by Elsevier Inc. on behalf of the AGA Institute. This is an open access article under the CC BY-NC-ND license (<http://creativecommons.org/licenses/by-nc-nd/4.0/>).

2352-345X

<https://doi.org/10.1016/j.jcmgh.2021.11.009>



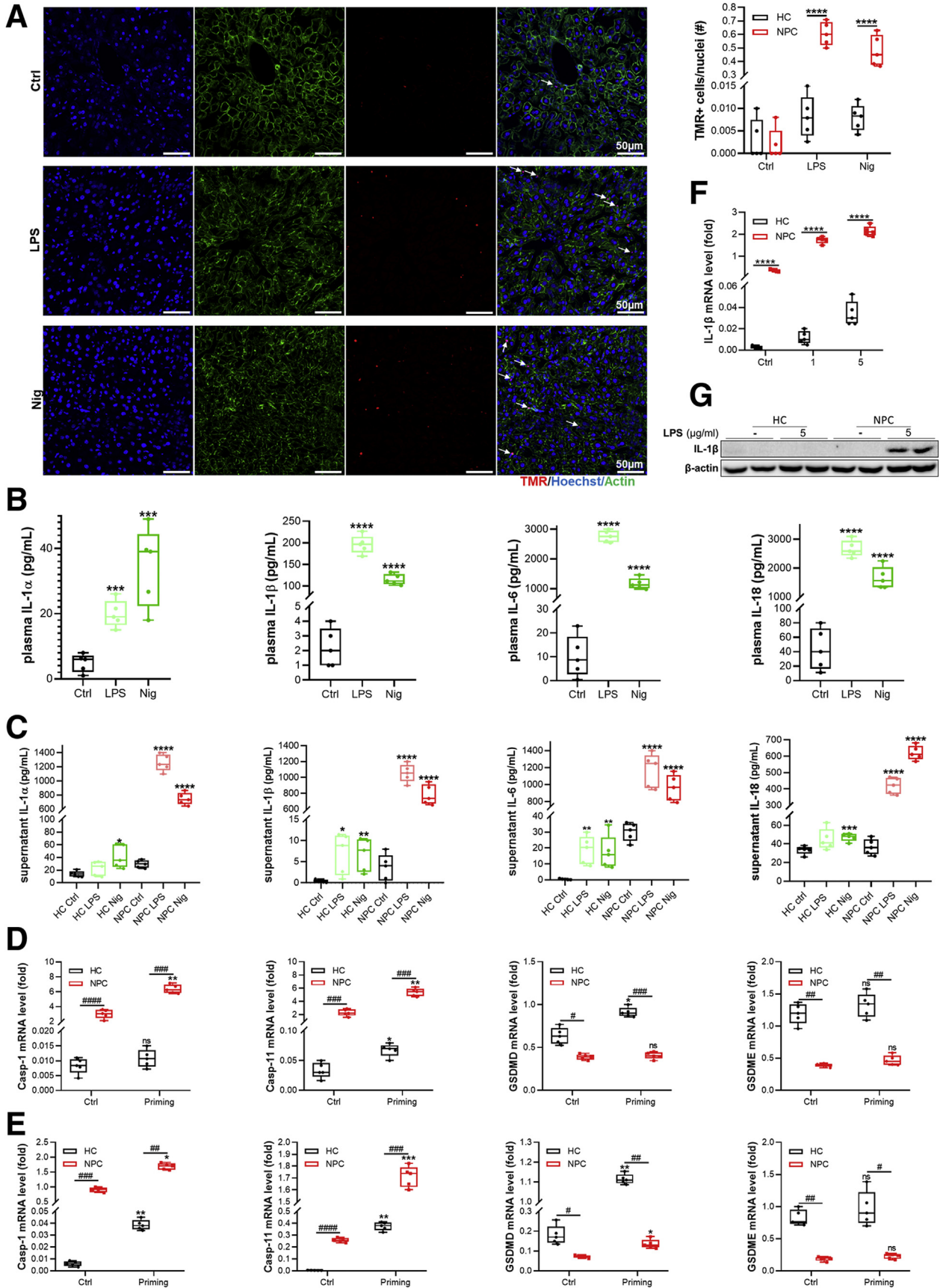
LPS-treated groups (Figure 1C and D). High concentrations (10 mmol/L) of nigericin, a potent NLRP3 inflammasome activator,²³ did increase LDH release significantly after 3 hours, but Western blot analysis showed significantly increased p-RIP1 levels instead of caspase-1 or GSDMD cleavage, suggesting cell death by necroptosis rather than pyroptosis or apoptosis (Figure 1C and D). High mobility group box 1 (HMGB1) can associate with LPS to improve its entry into cytosol in macrophages and endothelial cells.¹³ We therefore repeated the experiment this time by treating hepatocytes or nonparenchymal cells (NPC) of liver with LPS and HMGB1 together after overnight priming with LPS. LDH release was not increased in hepatocyte cultures, but LPS + HMGB1 did increase LDH release and GSDMD cleavage in NPC (Figure 1E and F). To assess the impact of NPC pyroptosis on liver cell death in vivo, assessed by aspartate aminotransferase (AST) and alanine aminotransferase (ALT) levels, we challenged WT mice with intraperitoneal LPS or nigericin after priming with intraperitoneal LPS for 12 hours. As shown in Figure 1G and H, plasma ALT and AST levels did not increase significantly (although did trend higher) compared with control (PBS-treated) mice. H&E staining of liver also did not show obvious cell death or structural damage in livers from LPS or nigericin-treated mice, but there were increased deoxyuridine-5'-triphosphate biotin nick end labeling-positive immune cells in liver, suggesting apoptosis or pyroptosis (Figure 2A), as well as increased plasma levels of interleukin (IL) 1 α , IL1 β , IL6, and IL18. As expected, in vitro studies showed very little cytokine release from hepatocytes but significantly increased cytokine release from NPCs in response to LPS or nigericin, which is consistent with activation of these cells and indicative of pyroptosis (Figure 2B and C). Finally, to determine a potential reason for hepatocyte resistance to pyroptosis, we assessed side-by-side protein levels of caspase-1/11, GSDMD/E in primary WT hepatocytes and NPC, with and without LPS priming for 6 hours. Expression of both caspase-1 and caspase-11 was not visible in hepatocytes, even after priming, when compared in the same Western blot with NPCs (Figure 1J). We can see both caspase-1 and caspase-11 activation with longer exposures

as shown in our previous studies, as well as the low level of mRNA of caspase-1 and caspase-11 even after priming in both in vitro and ex vivo studies (Figure 2D and E), suggesting only low level of expression. However, GSDMD levels were similar between hepatocytes and NPCs, with notably increased GSDME levels in NPCs after LPS priming. These findings, taken together, suggest that it is low expression of caspase-1/11 that renders hepatocytes resistant to pyroptosis.

Overexpression of Caspase-11 Active Domains Can Induce Hepatocyte Cell Death in Vitro

To test our hypothesis that low endogenous expression of caspase-1/11 in hepatocytes makes them resistant to lytic cell death after GSDMD cleavage, we overexpressed the p10 and p20 active domains of caspase-11 in primary isolated mouse hepatocytes using an adenovirus overexpression system. We initially attempted to prepare full-length caspase-11 adenovirus but found that significant autocleavage of caspase-11 occurred, which prevented production in a plasmid or virus system. We therefore prepared recombinant adenovirus-caspase-11-p10 and p20 separately and labeled them both with green fluorescent protein (GFP) (Figure 3A). Supernatant LDH and ALT levels did not increase significantly in control (empty vector virus) or with either p10 or p20 overexpression alone even up to 48 hours. However, with overexpression of both p10 and p20 caspase-11, both LDH and ALT levels increased significantly after 10 hours and peaked by 24 hours and also increased with increasing dose of p10/p20 overexpression (Figure 3B–D). As expected, hepatocytes did not release IL1 β despite significant levels of cell death (Figure 3E); meanwhile, IL1 β mRNA and IL1 β protein levels were much lower in hepatocytes compared with NPCs even after LPS treatment (Figure 2F and G), further indicating that hepatocytes are not a source of IL1 β even after caspase-1/11 activation. Western blot confirmed GFP-caspase-11 overexpression and associated cleavage of GSDMD, suggesting pyroptotic cell death (Figure 3F). We repeated the experiment using overexpression of caspase-1 p10 and p20 active

Figure 1. (See previous page). Hepatocytes are resistant to pyroptosis. Primary WT hepatocytes were isolated and primed with LPS (100 ng/mL) overnight, followed by stimulation with up to 10,000 ng/mL LPS for 16 hours. LDH release in cell supernatant (A) and caspase-11 (C11), cleaved caspase-11 (Cl-C11), GSDMD, and N-terminus GSDMD (N-GSDMD) levels in whole cell lysates by Western blot (B) were measured. LDH positive control (maximum level) was induced by 5 mmol/L H₂O₂ for 1 hour; β -actin was used as a loading control. Primary WT hepatocytes were primed by LPS (100 ng/mL) overnight and then stimulated with nigericin (Nig) or LPS (up to 10 μ g/mL) with or without transfection by LipofectamineP3000 (one reagent in the kit that may increase the transfection efficiency). LDH release in cell supernatant (C) and C11, Cl-C11, GSDMD, N-GSDMD, caspase-1 (C1), cleaved caspase-1 (Cl-C1), RIP1, and phospho-RIP1 (P-RIP1) levels in whole cell lysates by Western blot (D) were measured. (E) Relative LDH release from isolated primary WT hepatocytes and NPC primed by LPS (100 ng/mL) overnight and then stimulated by LPS (5 μ g/mL) \pm HMGB1 (400 ng/mL) for up to 24 hours. (F) Western blot of GSDMD and N-GSDMD levels from whole cell lysates of NPC primed by LPS (100 ng/mL) overnight and then stimulated by LPS (5 μ g/mL) \pm HMGB1 (400 ng/mL) for 16 hours. Plasma ALT (G) and AST (H) level from WT mice were treated with PBS (Ctrl) or primed with LPS (400 μ g/kg, intraperitoneal) for 6 hours, followed by either LPS (5 mg/kg, intraperitoneal) for 4 hours or nigericin (Nig; 3mg/kg, intraperitoneal for 2 hours. (I) H&E staining of liver tissue from the same groups of mice. Original magnification, \times 20 (left images), \times 40 for inset (right images). (J) C11, C1, GSDMD, and GSDME levels shown by Western blot of whole cell lysates from primary isolated hepatocytes or NPC from livers of WT mice 6 hours after priming with LPS (400 μ g/kg, intraperitoneal) or saline control. Data represent mean \pm SD. ** P < .01, **** P < .0001 vs control groups unless otherwise stated; n = 5 mice/group; β -actin is loading control. Images are representative across individual mice or across at least 3 independent experiments using cells from different mice.



fragments with similar results (Figure 3G and H). Finally, we isolated hepatocytes from caspase-11^{-/-} mice and repeated overexpression experiments with caspase-11-p10 and p20 with similar results, suggesting caspase-1/11 expression level regulates cell death and pyroptosis (Figure 3I and J).

We next wanted to characterize hepatocyte morphology in response to induced pyroptosis. Hepatocyte nuclei stained positive for propidium iodide and for TMR by 12 hours after infection with adenovirus caspase-11-p10+p20 (Figure 4A–D). Increased cell death was also shown by decreased mitochondrial staining with MitoTracker (Thermo Fisher Scientific, Waltham, MA) and decreased lysosomal staining with LysoTracker (Thermo Fisher Scientific) by 12 hours after induced overexpression of caspase-11-p10+p20 (Figure 4E). Interestingly, despite this evidence of increased cell membrane permeability, DNA cleavage, and cell death, the cell structure of the hepatocytes remained intact, as shown with phase contrast microscopy and retention of GFP within the cell (Figure 5A). Western blot analysis further confirmed cleaved GSDMD, release of HMGB1, and decreased actin and tubulin levels in pyroptotic hepatocytes, indicating release of cellular contents, with retention of lysosomal membrane protein LAMP2 and mitochondrial outer membrane protein TOM20 (Figure 5B). To determine morphologic changes over time, we used live-cell imaging, which shows cell death occurring by about 8 hours, but again cell structure and GFP retention at 24 hours (Figure 5C, Supplementary Video 1). We did observe ultrastructural changes within hepatocytes when imaged by electron microscopy, with atrophic mitochondria, dilated nuclear membrane, and dilated endoplasmic reticulum (Figure 5D). Taken together these data confirm pyroptotic cell death without overt cell rupture or effects to cell membrane structure.

Induced Hepatocyte Pyroptosis Is GSDMD-Dependent

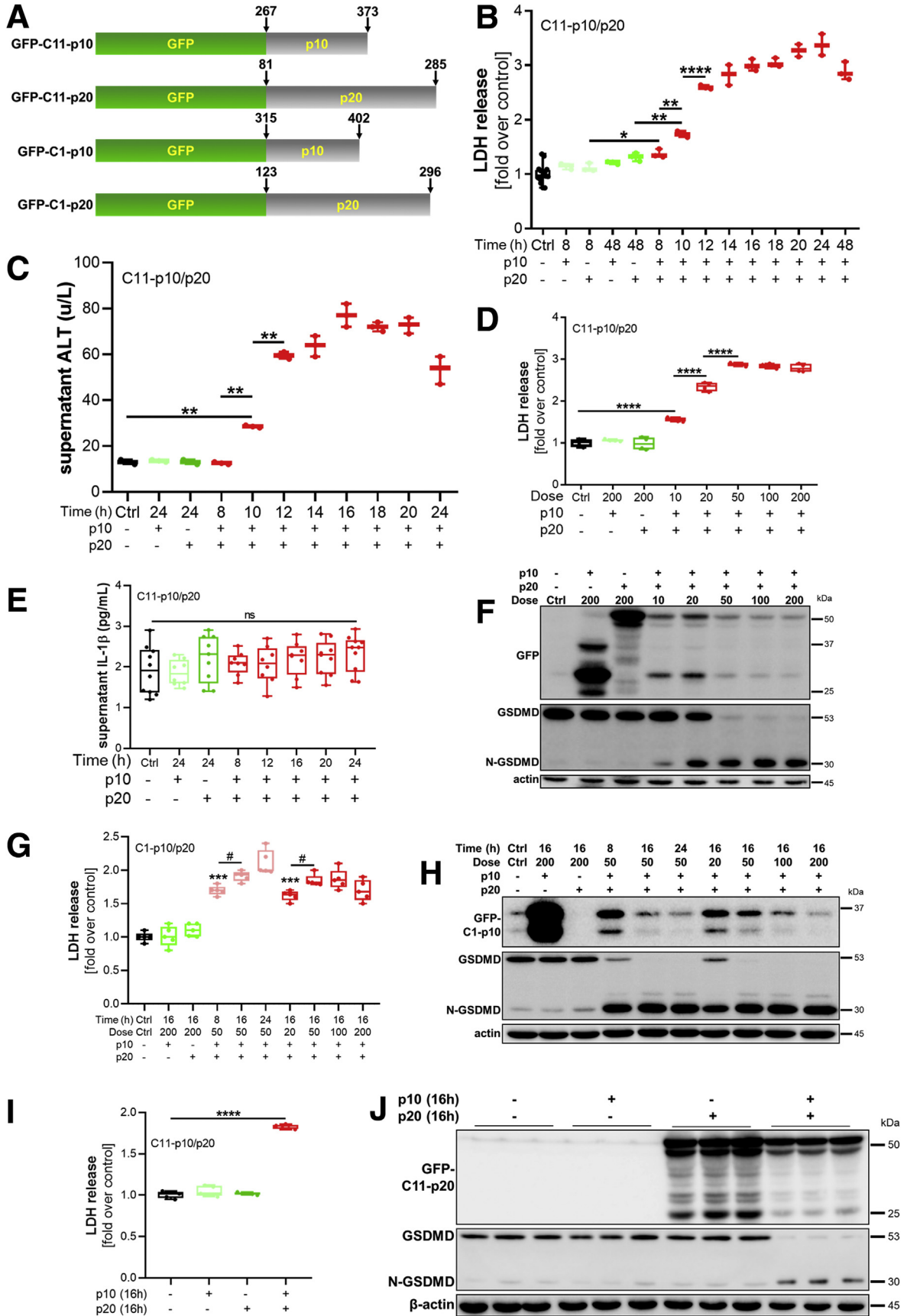
Cleavage of GSDMD is widely accepted as the main indicator of pyroptosis, and we showed increased GSDMD cleavage in hepatocytes overexpressing caspase-11p10+p20. However, other cell death pathways may still play a role, and eukaryotic cells have repair mechanisms that allow them to avoid pyroptosis even after cleavage of GSDMD.²⁴ Therefore, to more fully determine whether

induced hepatocyte cell death is truly GSDMD-dependent pyroptosis, we overexpressed caspase-11-p10+p20 in WT and GSDMD^{-/-} hepatocytes. LDH release increased significantly in WT cell culture but did not significantly change in GSDMD^{-/-} cell culture, suggesting GSDMD^{-/-} hepatocytes are resistant to lytic cell death (Figure 6A). Western blot analysis of cell lysates confirmed no GSDMD expression in knockout cells and confirmed overexpression of caspase-11p10 and p20. There were significantly increased levels of cleaved caspase-3 in GSDMD^{-/-} hepatocytes at later time points after caspase-11-p10+p20 overexpression (Figure 6B). Because caspase-3 can also cleave GSDME to mediate pyroptosis,⁷ we measured GSDME expression and cleavage. We did not observe increased GSDME expression or increased GSDME cleavage, suggesting any hepatocyte cell death was more likely apoptosis rather than pyroptosis (Figure 6B). We confirmed increased apoptotic morphology (cell shrinkage, nuclear condensation and fragmentation, propidium iodide positive staining, concentrated exogenous GFP) in GSDMD^{-/-} hepatocytes at later time points after overexpression of caspase-11-p10+p20 (Figure 6C, Supplementary Video 2). To further confirm the dependence of induced hepatocyte cell death on GSDMD, we overexpressed GSDMD in a subset of GSDMD^{-/-} hepatocytes for 24 hours, followed by overexpression of caspase-11-p10+p20. Expressing GSDMD in GSDMD^{-/-} cells increased LDH release in cell culture and increased TMR-positive cells (Figure 6D). Western blot analysis confirmed effective caspase-11 and/or GSDMD expression and cleavage and normalization of cleaved caspase-3 levels (Figure 6E). Confocal immunofluorescence imaging also confirmed TMR positivity and cell death after overexpression of GSDMD in GSDMD^{-/-} hepatocytes (Figure 6F).

Caspase-11-P10+P20 Induces Hepatocyte Pyroptosis in Liver in Vivo and Is Also GSDMD-Dependent

Having shown that pyroptosis can be induced in hepatocytes in vitro with overexpression of caspase-1/11 active fragments, we next wanted to determine whether we could similarly induce these effects in vivo, and whether there were changes to liver cell morphology. We injected WT and GSDMD^{-/-} mice with adenoviral caspase-11-p10/p20 via tail vein and assessed plasma AST and ALT as markers of

Figure 2. (See previous page). Hepatocytes are resistant to pyroptosis mainly because of low level of caspase-1/11. (A) Immunofluorescence images of TMR-red staining of liver tissue from WT mice treated with PBS (Ctrl) or primed with LPS (400 μ g/kg intravenous) for 6 hours, followed by either LPS (5 mg/kg intravenous) for 4 hours or Nig (3 mg/kg intravenous) for 2 hours. TMR, red; Hoescht nuclear stain, blue; actin, green. (B) Plasma IL1 α , IL1 β , IL6, and IL18 levels from similar groups of WT mice. (C) Supernatant IL1 α , IL1 β , IL6, and IL18 levels from isolated primary WT hepatocyte or NPC cultures primed by LPS (100 ng/mL) overnight and then stimulated by LPS (5 μ g/mL, 16 hours) or nigericin (10 μ mol/L, 3 hours). Ctrl group treated with same volume of solvent. (D) mRNA level of related proteins from isolated primary WT hepatocyte or NPC with or without priming in vitro by LPS (100 ng/mL) overnight. (E) WT mice treated with PBS (Ctrl) or primed with LPS (400 μ g/kg intravenous) for 6 hours. Then mRNA levels of related proteins from isolated primary WT hepatocytes or NPC were detected. (F and G) mRNA and protein levels of IL1 β from isolated primary WT hepatocytes and NPC primed by LPS (100 ng/mL) overnight and then stimulated by LPS (1–5 μ g/mL) for 16 hours. Data represent mean \pm SD. */#P < .05, **/###P < .01, ***/####P < .001, ****/#####P < .0001 vs respective Ctrl group unless specified; n = 5 mice/group. Images are representative across individual mice.



hepatocyte damage at 8 hours. Hepatocytes possess a high affinity adenovirus receptor that is not present on NPCs, so adenovirus is often used to overexpress proteins in hepatocytes.²⁵ Plasma ALT and AST levels increased slightly in WT mice after adenoviral transfection of caspase-11-p10 or p20 alone by 8 hours but was dramatically and significantly increased by 8 hours with both p10 and p20 expression, with little increase in GSDMD^{-/-} mice at this time (Figure 7A, left and middle). Nearly all the WT mice died within 24 hours of injection, but all the GSDMD^{-/-} mice survived until 48 hours (Figure 7A, right). We got similar results in WT mice injected with adenoviral caspase-1-p10+p20 (Figure 7B), with Western blot analysis of whole liver lysates confirming caspase-1 overexpression and also confirming increased cleavage of GSDMD (Figure 7B). Interestingly, liver function deteriorated significantly at 24 hours in GSDMD^{-/-} mice given caspase-11-p10+p20 (Figure 7A, left). Similarly to our in vitro experiments, we found that GSDMD^{-/-} mice showed a compensatory increase in hepatocyte apoptosis at 24 hours, as shown by increased levels of cleaved caspase-3 (Figure 7C). We further confirmed the role of GSDMD in vivo, as we had previously in vitro, by treating GSDMD^{-/-} mice with recombinant adenovirus-GSDMD for 24 hours before administration of caspase-11-p10+p20. As expected, mice expressing GSDMD had increased plasma ALT levels at 8 hours and increased TMR-positive cells (Figure 7D). GSDMD cleavage was confirmed by Western blot of whole liver cell lysates as previously (Figure 7D).

H&E staining of liver demonstrated significant areas of cell death in WT mice injected with caspase-11-p10+p20, including significant perilobular necrosis (Figure 8A). There was also significant hepatocyte TMR-positive staining shown by immunofluorescence (Figure 8A). CD45⁺ immunohistochemical staining of livers also revealed significantly increased immune cell infiltration in WT mice given caspase-11-p10+p20 (Figure 8A). No cell death or obvious immune cell infiltration was observed in livers of GSDMD^{-/-} mice given caspase-11-p10+p20 for 8 hours. However, the picture changed by 24 hours in these GSDMD^{-/-} mice, with large areas of cell death and TMR-positive cells (Figure 8A). More detailed examination of the H&E staining of these livers suggested apoptotic cell death morphology at 24 hours in GSDMD^{-/-} mice, with reduced cell volume,

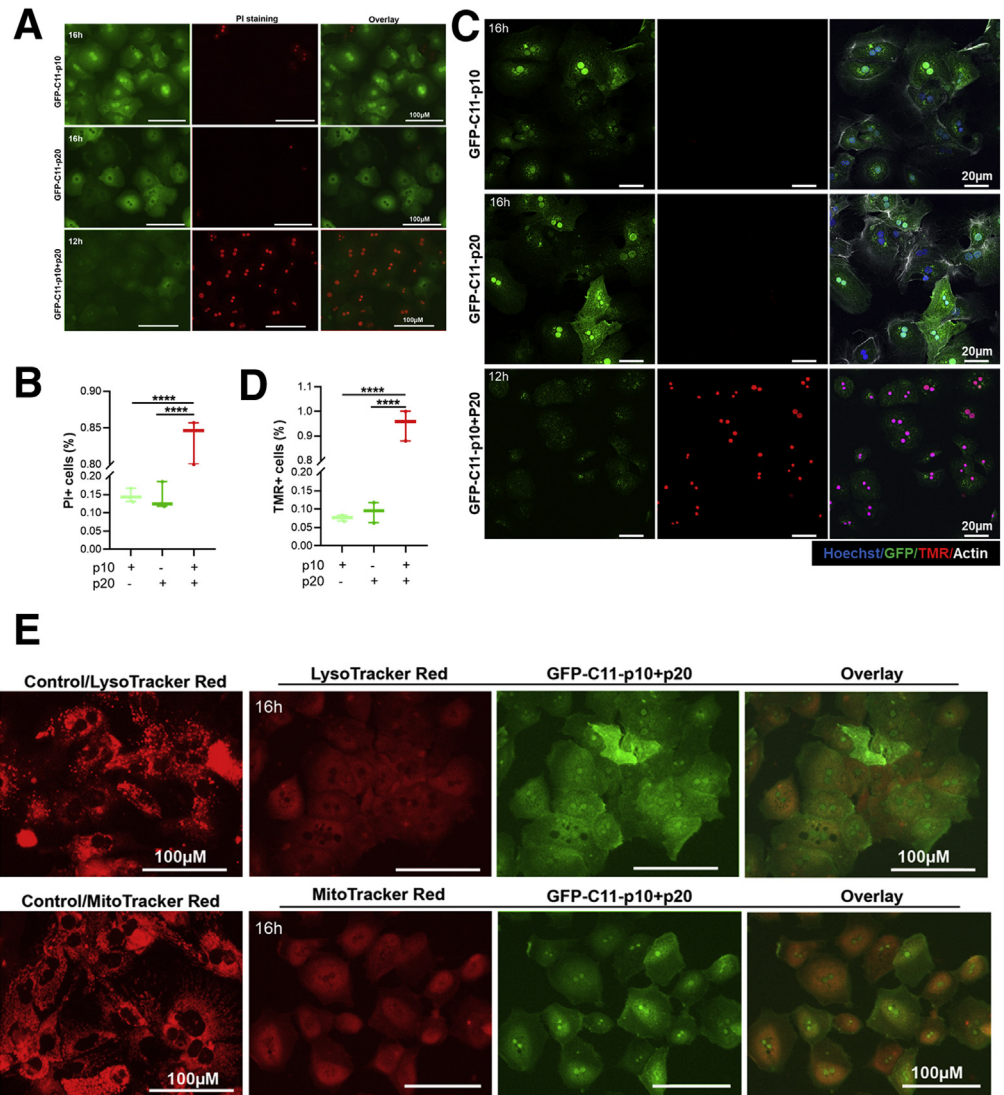
increased eosinophilic plasma, and condensed nuclei. Infiltrating immune cells were also much fewer than in WT groups (Figure 8A).

We also investigated ultrastructural changes in liver using electron microscopy. Images of pyroptotic hepatocytes revealed chromatin margination in the nucleus, dilated nuclear membrane, endoplasmic reticulum dilation and fragmentation, and increased numbers of ribosome-bearing vacuoles likely originating from fragmented endoplasmic reticulum (Figure 8B).

Discussion

Pyroptosis is a recently defined form of RCD where cleavage of GSDMD is the executor.^{4,5} Pyroptosis is obvious in macrophages, with activation of caspase-1 or -11 resulting in rapid lytic cell death from GSDMD pores in the cell membrane. However, whether pyroptosis similarly occurs in hepatocytes (and other epithelial cells) is still largely controversial, because these cells do not exhibit the rapid cell rupture and release of contents seen in macrophages. Previously published data supported hepatocyte pyroptosis, as defined by caspase-1/11 activation, positive staining with propidium iodide, and even release of IL1 β in some studies. However, in these studies cleaved GSDMD was not detected, or typical morphology of pyroptosis was not shown,^{14-17,26-42} or other forms of RCD, such as apoptosis or necroptosis, were not excluded.⁴³ Similarly, there are also extensive data, including from our group, suggesting activated caspase-1 or -11 does not lead to lytic cell death. We found that caspase-1 activation is actually hepatoprotective in a model of oxidative stress through the up-regulation of beclin1 and mitochondrial autophagy.^{18,19} We also determined that caspase-11/GSDMD mediates exosomal HMGB1 release from hepatocytes during sepsis, an active process rather than passive release via cell death and cell rupture.^{13,21} Our current study revealed that activation/stimulation of endogenous caspase-1 or -11 was unable to induce lytic cell death, despite inducing low levels of GSDMD cleavage. This relatively low expression of caspase-1 and -11 in hepatocytes compared with NPCs, and subsequent low GSDMD cleavage levels, may also explain our previous results showing a protective effect of caspase-1 activation in ischemia/hypoxia injury¹⁸ and active release of HMGB1 after LPS stimulation and caspase-11 activation^{13,21} rather

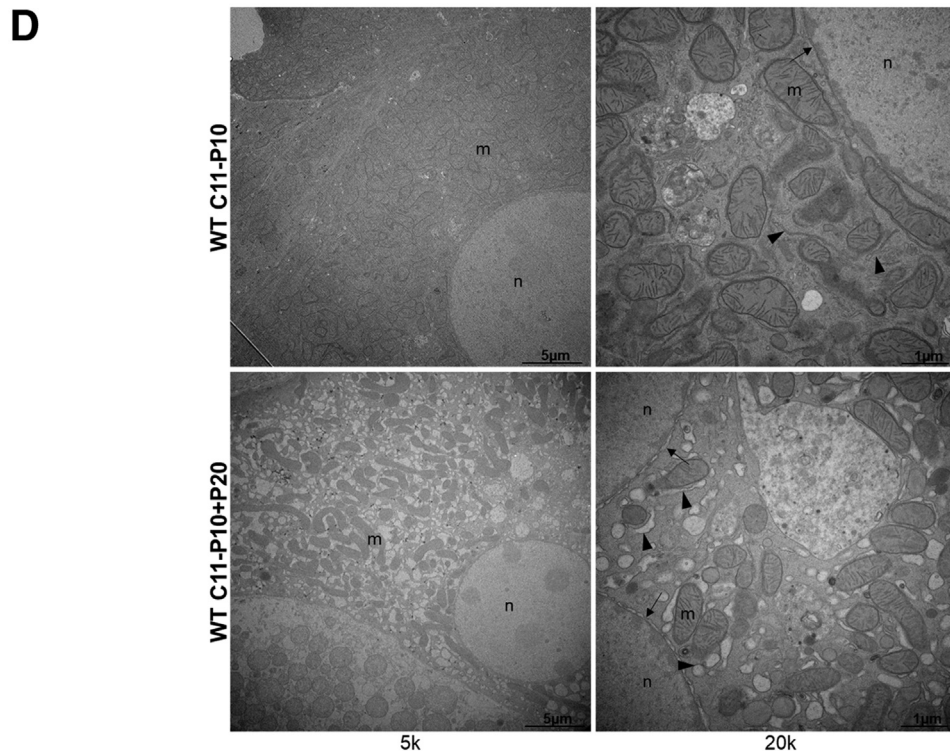
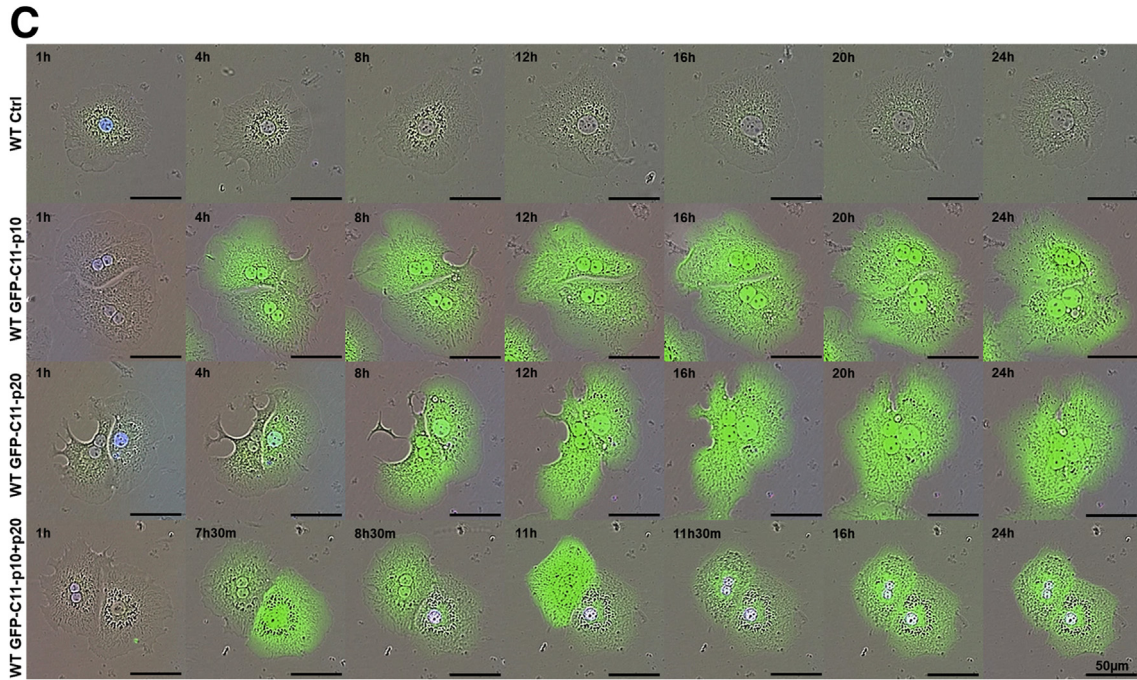
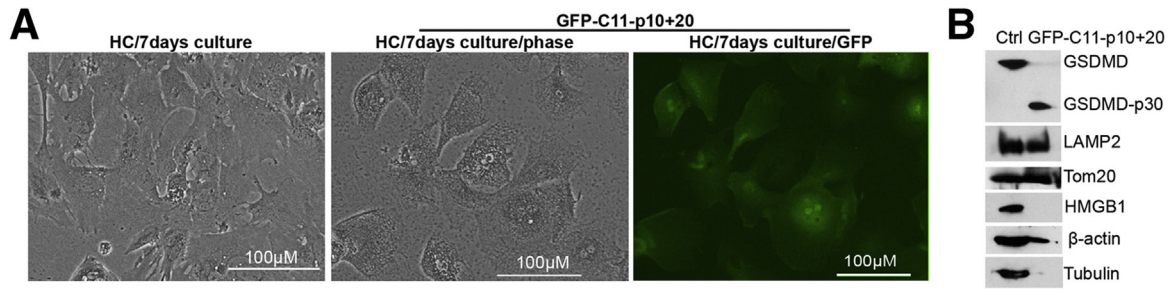
Figure 3. (See previous page). Overexpression of caspase-11 active domains can induce hepatocyte cell death in vitro. (A) Schematic of vector construction for GFP-labeled p10 and p20 (active) fragments of caspase-11 (C11) and caspase-1 (C1) expression vector construction. Numbered arrows refer to amino acid sequence from full-length proteins. Relative LDH release (B) and supernatant ALT (C) in isolated primary WT hepatocyte culture after treatment with Ad-GFP-C11-p10 or p20 alone or together at a dose of 200 VP/cell for indicated period of time. Relative LDH level (D) in supernatant of WT hepatocyte culture after treatment with Ad-GFP-C11-p10 or p20 alone or together for 16 hours at indicated dose (VP/cell). (E) IL1 β levels in similar groups of WT hepatocytes as indicated. (F) Western blot of whole cell lysates of similar groups of hepatocytes showing GFP, GSDMD, and N-GSDMD expression. Relative LDH release (G) in isolated primary WT hepatocyte culture treated by Ad-GFP-C11-p10 or p20 alone or together at a dose of 50 VP/cell for indicated period of time or for 16 hours at indicated dose (VP/cell). (H) Western blot of whole cell lysates of similar groups of hepatocytes showing GFP, GSDMD, and N-GSDMD expression. Relative LDH release in supernatant (I) or (J) Western blot showing GFP, GSDMD, and N-GSDMD of whole cell lysates of caspase-11^{-/-} hepatocytes treated by Ad-GFP-C11-p10 or p20 alone or together at a dose of 50 VP/cell for 16 hours. Data represent mean \pm SD. */ $\#P < .05$, ** $P < .01$, *** $P < .001$, **** $P < .0001$ vs control groups unless otherwise stated; β -actin is loading control. All data are representative of 3 independent experiments using cells from different mice.



than lytic cell death in hepatocytes. Contrary to some other studies, we also do not detect a function for caspase-1 or caspase-11 in cytokine maturation in hepatocytes, which is similar to our and others' previous findings that caspase-1 in particular mediates other functions rather than pyroptosis and cytokine maturation.⁴⁴

Because of the relative differences in function between immune cells such as macrophages/monocytes and epithelial cells such as hepatocytes, it is not altogether surprising that they have different tolerances to induction of cell death. Macrophage production of potentially harmful inflammatory cytokines needs to be closely regulated, and so induction of inflammasome pathways and activation and release of IL1 β in these cells could understandably result in rapid cell death. However, epithelial cells such as hepatocytes and gut epithelia are often long-lived with multiple functions

unrelated to inflammation and innate immune responses. Hepatocytes in particular provide the main structure for the liver and have a variety of vital functions in metabolism and production of vital proteins. Therefore, it makes sense that hepatocytes would be somewhat resistant to cell death including pyroptosis. Our findings that hepatocyte cell structure is maintained are interesting and potentially suggest not only the importance of the structural role for these cells but also the possibility of involvement in repair and regeneration of the liver by providing a still intact scaffold. This is obviously speculation that will need to be backed up by experimental data, but the findings are nonetheless thought-provoking. Because robust evidence showed that nerve injury-induced protein 1 (NINJ1) mediated plasma membrane rupture in lytic cell death including pyroptosis after gasdermin pore formation in



macrophages,⁴⁵ we also explored the role of NINJ1 in hepatocyte pyroptosis but failed to detect the expression of NINJ1 in hepatocytes (Figure 8C). Maybe other pathways other than NINJ1 mediate hepatocyte pyroptosis downstream of pore formation. These contrary results between different cells are worthy of further exploration.

Another interesting concept has emerged recently wherein hepatocytes and inflammasome signaling in hepatocytes are drivers, potentiators, and possibly regulators of immune and inflammatory responses. Published data from our group have already described hepatocyte caspase-11-mediated release of exosomes containing HMGB1 as main drivers of macrophage pyroptosis in sepsis.^{13,21} Similarly, inflammasome activation in hepatocytes can induce activation of pyroptotic signaling and release of inflammasome components that can activate hepatic stellate cells to induce fibrotic reactions¹⁷ or to activate NLRP3 inflammasome in Kupffer cells and trigger nonalcoholic steatohepatitis.⁴² These findings strongly suggest additional roles for inflammasome and pyroptosis signaling in hepatocytes and other epithelial cells that are not present in immune cells.

In summary, our data shown here confirm activation of canonical and non-canonical inflammasome pathways with appropriate stimuli and downstream activation of GSDMD. However, hepatocytes are resistant to pyroptosis primarily through low expression levels of caspase-1 or -11, which are insufficient to cleave sufficient GSDMD to cause cell lysis through membrane pore formation. However, there does appear to be sufficient activity to have alternative effects in hepatocytes such as release of HMGB1 or inflammasome components. Further studies are needed to more fully elucidate additional pathways involved in alternative inflammasome functions in hepatocytes and how these pathways contribute to liver pathology and disease.

Materials and Methods

Animals and Animal Models

GSDMD and caspase-11 knockout (KO; GSDMD^{-/-} and Casp-11^{-/-}) mice on a C57BL/6 background were bred and housed under specific pathogen-free conditions in our facility. C57BL/6 (WT) controls were purchased from The Jackson Laboratory (Bar Harbor, ME). Littermates were co-housed for at least 7 days before experimentation. Male mice aged 8–12 weeks, weighing 25–30 g, were used in experiments. All experimental protocols were approved by the Institutional Animal Use and Care Committee of the

University of Pittsburgh, and all the experiments were performed in accordance with National Institutes of Health guidelines for the use of laboratory animals.

Endotoxemia ± nigericin. Mice were primed with injection of intraperitoneal low-dose LPS (400 µg/kg) for 6 hours, followed by challenge with high-dose LPS (5 mg/kg) for 4 hours, or nigericin (3 mg/kg) for 2 hours, or same volume of respective solvent as control. For ex vivo study, mice were just primed with same dose of LPS or solvent for 6 hours, followed by primary hepatocyte and NPC cell isolation and detection.

GSDMD overexpression. Recombinant adenoviral-GSDMD or empty vector control at a dose of 1*10¹⁰ virus particles (VP)/mouse in 200 µL volume was injected via caudal vein 24 hours before experimentation.

Caspase-1 or 11 p10 and/or p20 overexpression. Recombinant adenoviral-caspase-1-p10, caspase-1-p20, caspase-11-p10, or caspase-11-p20 or empty vector controls at a dose of 1*10¹⁰ VP/mouse in 200 µL volume were injected via caudal vein 24 hours before experimentation. In some experimental groups caspase-1-p10 and p20 or caspase-11 p10 and p20 were injected together at the same doses in a total volume of 200 µL.

Expression Vector Construction

The cDNA vectors of caspase-11 and caspase-1 were from OriGene (Rockville, MD). GFP open reading frame without stop codon was inserted into a serotype 5-based adenoviral shuttle vector.⁴⁶ The cytomegalovirus major immediate-early promoter drives caspase-1/11 expression. Caspase-11-p10 (267-373 amino acid coding region with a stop codon), p20 (81-285 amino acid coding region with a stop codon), caspase-1-p10 (315-402 amino acid coding region with a stop codon), or p20 (123-296 amino acid region with a stop codon) was amplified from caspase-11 or caspase-1 cDNA vector by polymerase chain reaction and inserted at the C terminus of GFP open reading frame to generate a fusion open reading frame. All inserted genes were sequencing verified. Adenoviral vectors were generated and purified as described.^{46,47}

Reagents

Anti-cleaved caspase-3 antibody, anti-caspase-3 antibody, anti-β-actin antibody, anti-RIP1 (receptor-interacting protein 1) antibody, anti-p-RIP1 (phospho-RIP1) antibody, cell lysis buffer (10×), and protease/phosphatase inhibitor cocktail were all from Cell Signaling Technology (Danvers,

Figure 5. (See previous page). Morphologic features of induced hepatocyte pyroptosis in vitro. (A) Phase contrast images and immunofluorescence of isolated primary WT hepatocytes treated with Ad-GFP-C11-p10 alone as control or together with p20 at a dose of 100 VP/cell for 7 days. (B) Western blot of whole cell lysates from similar groups of hepatocytes showing GSDMD, N-GSDMD, LAMP2, Tom20, HMGB1, β-actin, and tubulin expression. (C) Living cell images taken over 24 hours of isolated primary WT hepatocytes treated by GFP-C11-p10 or p20 alone or together at a dose of 100 VP/cell. GFP, green. Original magnification, ×40. (D) Transmission electron microscopy images of isolated primary WT hepatocytes treated with GFP-C11-p10 alone or together with p20 at a dose of 100 VP/cell for 6 hours. Atrophic mitochondria, dilated nuclear membrane, and endoplasmic reticulum were observed during the process of HC death. m, mitochondria; n, nucleus; arrow, nuclear membrane; arrowhead, endoplasmic reticulum. Original magnification, ×5000 (5k) or ×20,000 (20k). All data are representative of 3 independent experiments using cells from different mice.

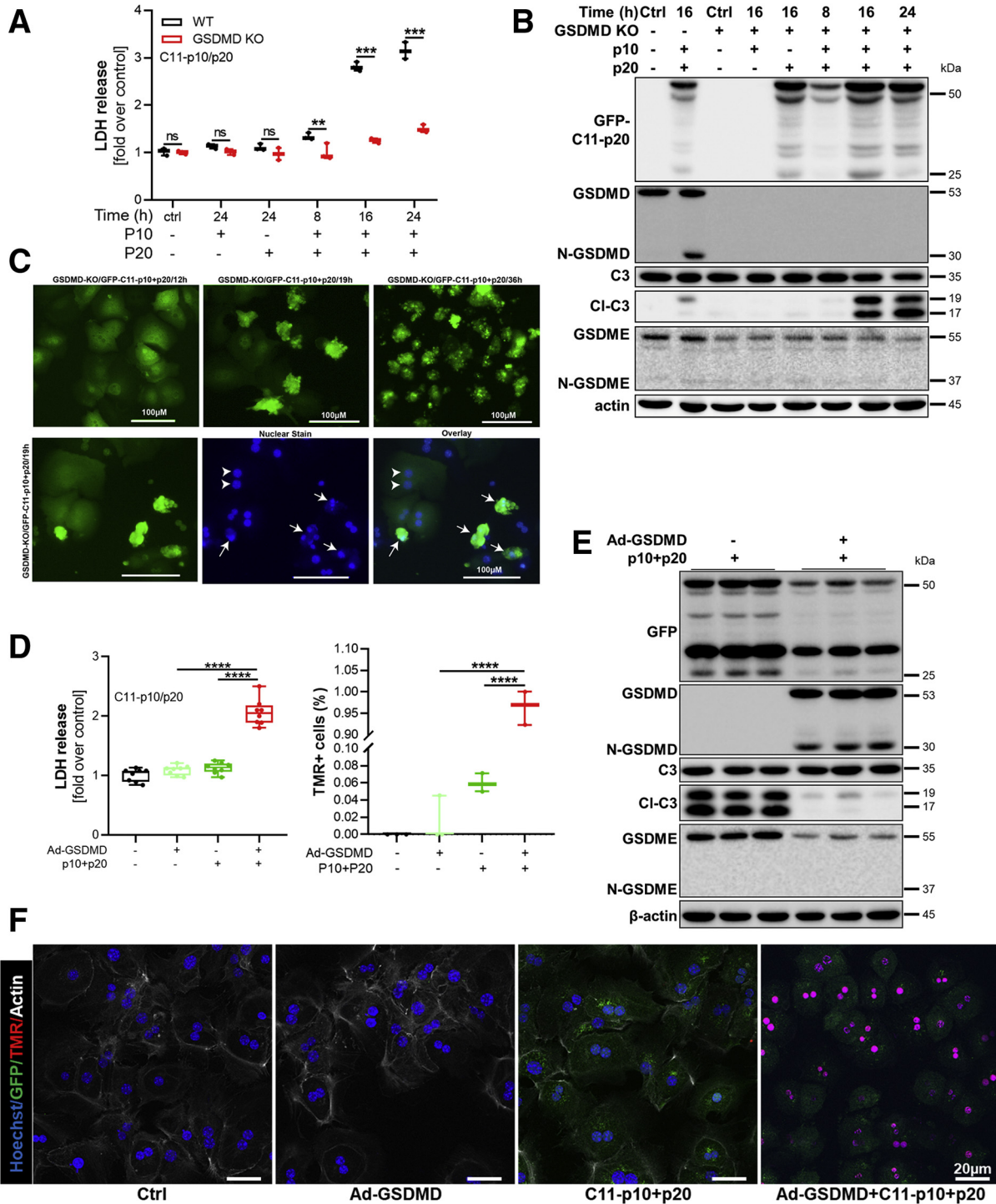
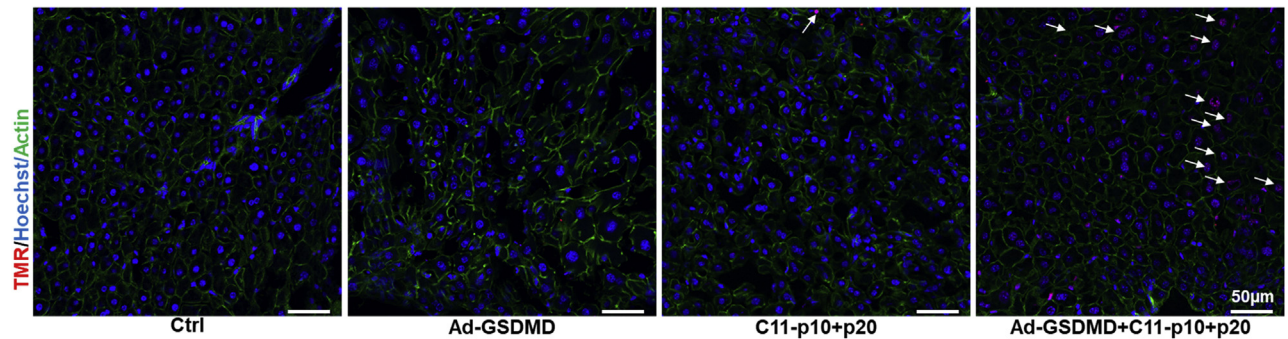
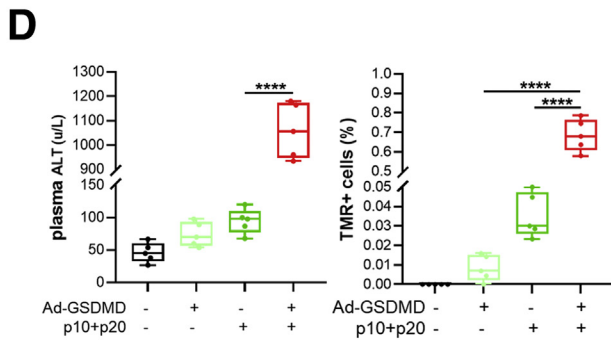
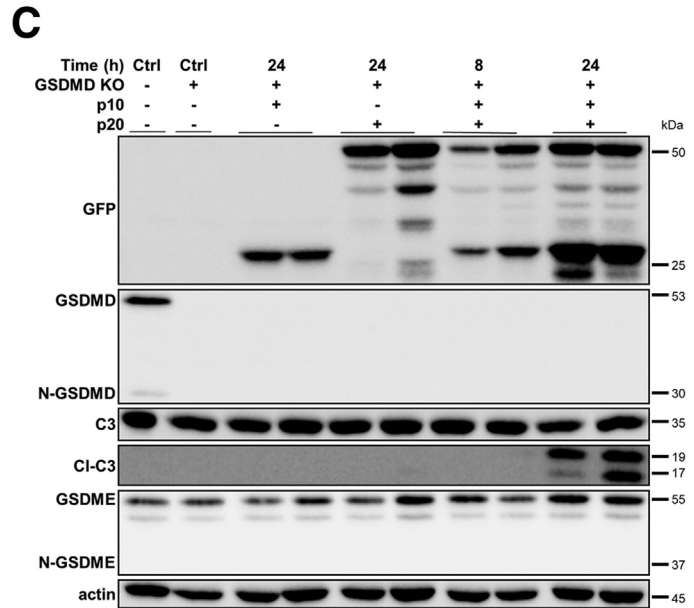
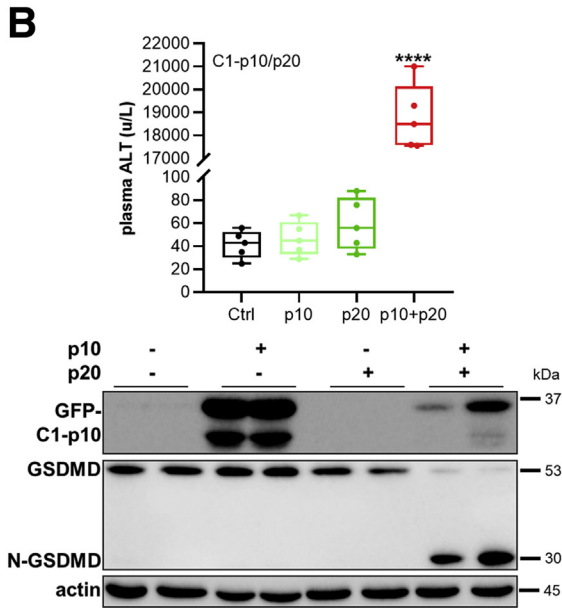
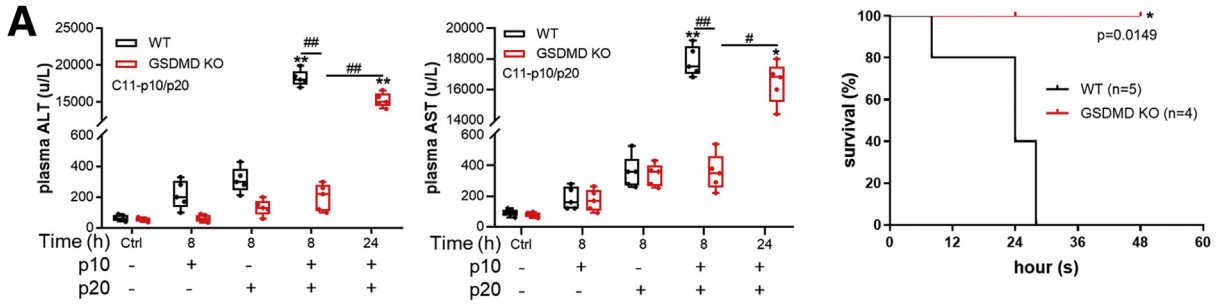


Figure 6. Induced hepatocyte pyroptosis is GSDMD-dependent. Relative LDH release (A) and (B) Western blot of whole cell lysates of isolated primary WT and GSDMD^{-/-} hepatocytes treated with Ad-GFP-C11-p10 or p20 alone or together, or control empty vector adenovirus (Ctrl), at a dose of 100 VP/cell for indicated time points showing expression of GFP, GSDMD, N-GSDMD, caspase-3 (C3), cleaved caspase-3 (CI-C3), GSDME, and N-GSDME. (C) Immunofluorescence (IF) images of isolated primary GSDMD^{-/-} hepatocytes treated with Ad-GFP-C11-p10 and p20 together at a dose of 100 VP/cell for indicated period of time (Arrowhead = normal hepatocyte nuclei; Arrow = apoptotic nuclei). (D) Relative LDH release and TMR-red positive staining of isolated primary GSDMD^{-/-} hepatocytes transfected with Ad-GSDMD for 24 hours with/without caspase-11 (C11)-p10 + p20 for 16 hours at a dose of 100 VP/cell. (E) Western blot of whole cell lysates of primary hepatocytes from similar groups showing expression of GFP, GSDMD, N-GSDMD, C3, CI-C3, GSDME, and N-GSDME levels. (F) IF of isolated primary GSDMD^{-/-} hepatocytes treated with Ad-GSDMD for 24 hours with/without C11-p10 + p20 for 16 hours at a dose of 100 VP/cell. Hoescht nuclear stain, blue; TMR, red; GFP, green; actin, white. Data represent mean ± SD. **P < .01, ***P < .001, ****P < .0001. Original magnification, ×40. All data are representative of 3 independent experiments using cells from different mice.



MA). Anti-caspase-11 antibody, anti-pro caspase-1+p10+p12 antibody, anti-GSDMD antibody, anti-GSDME antibody, and propidium iodide were from Abcam (Cambridge, UK). Anti-GFP antibody, Hoechst 33342, MitoTracker Deep Red FM, and LysoTracker Deep Red were from Invitrogen. Anti-F4/80 antibody was from BD Biosciences (Franklin Lakes, NJ). TMR red kit was from Roche (Basel, Switzerland). Lipofectamine 3000 Transfection Reagent was from Thermo Fisher Scientific.

Primary Hepatocyte and NPC Isolation and Treatment

Hepatocytes were isolated by a modified in situ collagenase (type VI; Sigma-Aldrich, St Louis, MO) perfusion technique as previously described.⁴⁸ Hepatocyte purity exceeded 99% measured by flow cytometry, and viability is typically over 95% verified by trypan blue. NPCs were purified by differential centrifugation to remove hepatocytes. Hepatocytes (2×10^6 cells/6 cm-plate) were plated on gelatin-coated plates, and NPCs were plated directly in Williams-E medium with 10% calf serum, 1 μ mol/L humulin, 15 mmol/L HEPES, 2 mmol/L L-glutamine, 100 U/mL streptomycin, and 100 U/mL penicillin. Cells were allowed to attach overnight, and then the medium was changed before treatment. Cells were primed with LPS (100 ng/mL) overnight and then stimulated by nigericin (10 μ mol/L), LPS (100 ng/mL), or LPS (100 ng/mL) + HMGB1 (400 ng/mL), or transfected with LPS by Lipofectamine 3000 according to manufacturer's protocol. For adenoviral overexpression, empty vector or adenovirus containing recombinant protein was added to the medium directly, and medium was changed every 2-3 days.

Liver Function and Cytokine Abundance Assessment

ALT and AST levels were detected by the DRI-CHEM 4000 Chemistry Analyzer System (Heska, Loveland, CO) according to the manufacturer's instructions. Cytokine abundance was measured by enzyme-linked immunosorbent assay according to the protocol with Mouse IL1 β DuoSet ELISA, IL1 β DuoSet ELISA, IL6 DuoSet ELISA from

R&D Systems (Minneapolis, MN). IL18 Mouse ELISA Kit was from Invitrogen.

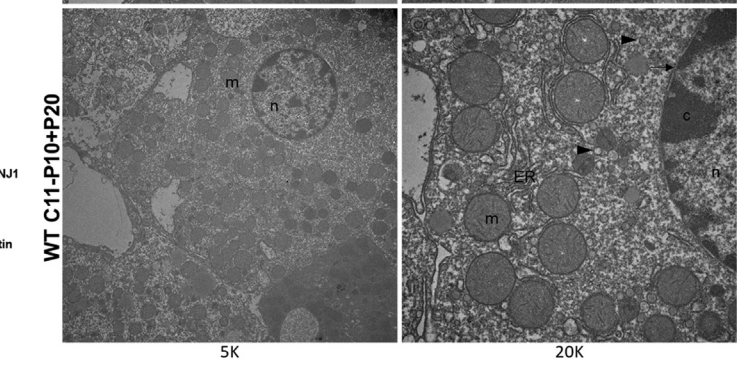
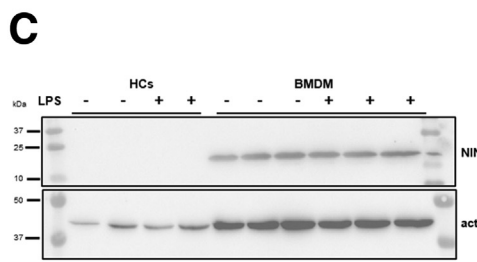
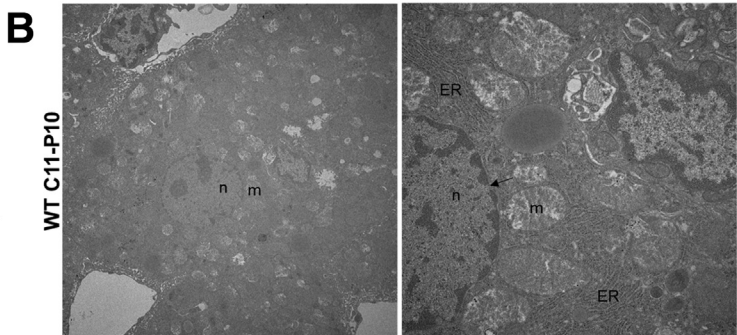
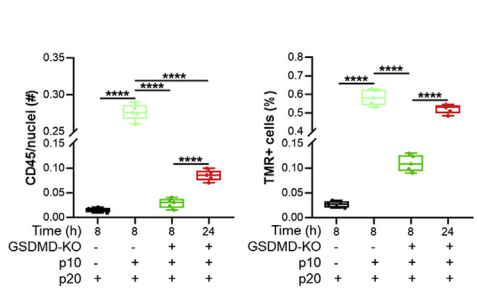
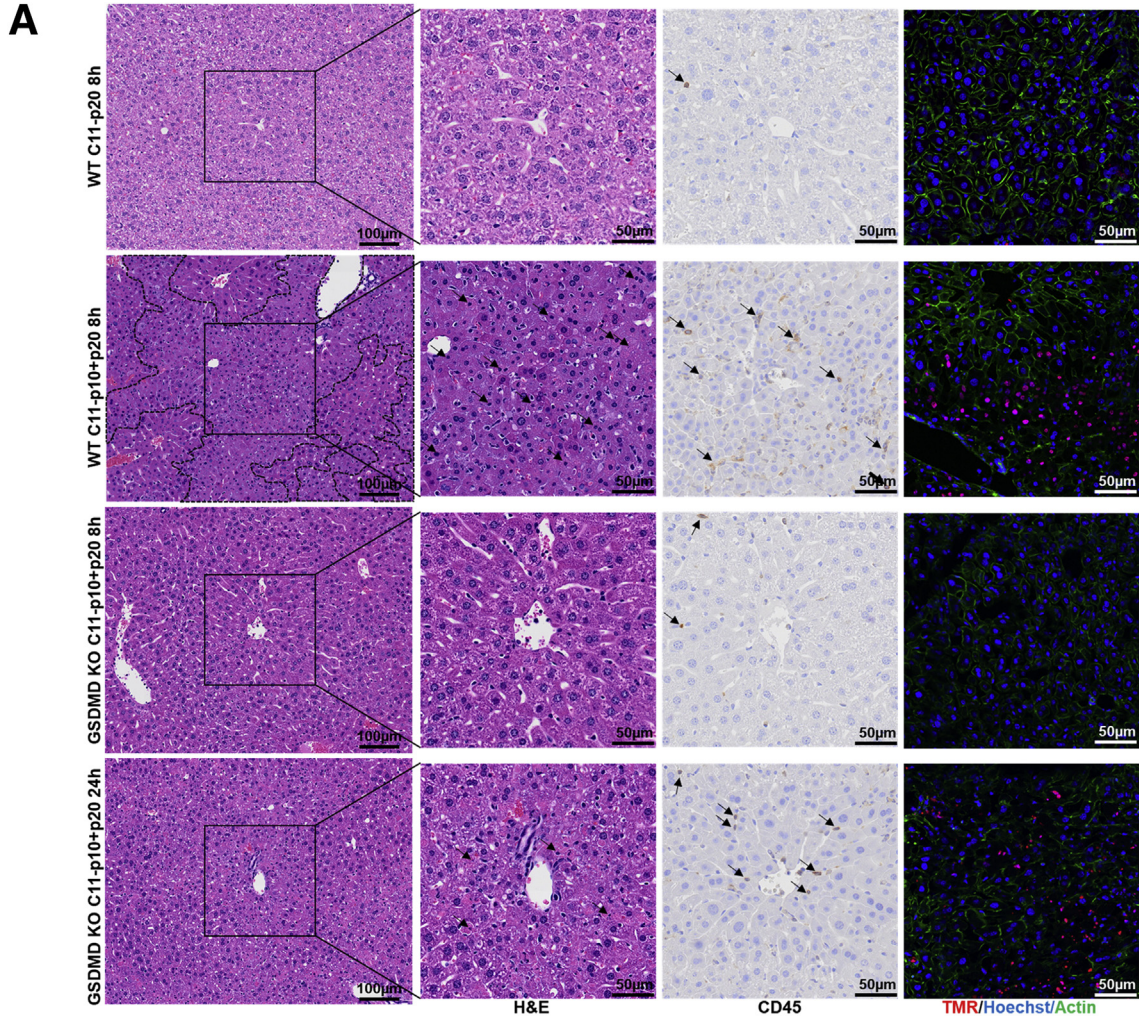
H&E, Immunohistochemistry, and Immunofluorescence Staining

Tissue samples were prepared for H&E and IF staining by methods as described by our group previously.⁴⁹ Samples were imaged at the Center for Biologic Imaging (University of Pittsburgh). Tissue samples were prepared for immunohistochemistry (IHC) staining by standard principles and methods of IHC as described.⁵⁰ Briefly, after removal of blood by cardiac puncture, mice are perfused with cold PBS to remove red blood cells left in tissues and circulation. Next, mice are perfused with 2% cold paraformaldehyde, followed by harvest of the tissue and placement in 5 mL 2% cold paraformaldehyde for 2 hours at 4°C. Half of the tissue is then switched over to 70% ethanol (H&E and IHC), with the other half placed in 30% sucrose (immunofluorescence) replaced 3 times over a 24-hour period. H&E and IHC staining was performed by Pitt Biospecimen Core. For IHC staining, tissues underwent antigen retrieval, blocking, incubation of primary (Anti-CD45 Rabbit mAb, Cell Signaling Technology) and secondary antibodies, addition of chromogenic agents, dehydration, and sealing with coverslip after deparaffinizing. For immunofluorescence staining, tissues are frozen with liquid nitrogen-cooled 2-methylbutane. Tissues sections (6 μ m) were permeabilized with 0.3% Triton X-100 for 20 minutes and stained for cell death with In Situ Cell Death Detection TMR Red as described previously.⁴⁹ Imaging conditions were maintained at identical settings for each antibody-labeling experiment. Large-area images equivalent to 9 unique fields taken by NikonA1 (Tokyo, Japan) confocal microscope (purchased with NIH grant 1S100D019973-01, PI: Dr Simon C. Watkins). Quantitation was performed using ImageJ (NIH).

Transmission Electron Microscopy

For electron microscopy experiments, mice were euthanized and then perfused with ~20 mL cold PBS to wash out all the blood, followed by perfusion with 10 mL of 2.5% glutaraldehyde in 0.1 mol/L phosphate buffer (pH 7.4), and

Figure 7. (See previous page). Caspase-11-p10 + p20 induces hepatocyte pyroptosis in liver in vivo and is also GSDMD-dependent. (A) Plasma ALT and AST levels in WT and GSDMD^{-/-} mice treated with Ad-GFP-C11-p10 or p20 alone or together at a dose of 1×10^{10} VP/mouse for time points up to 24 hours and 5-day survival of similarly treated groups of mice. (B) Plasma ALT levels and Western blot showing expression of GFP, GSDMD, and N-GSDMD in whole cell liver lysates of WT mice treated with Ad-GFP-caspase-1-p10 or p20 alone or together at a dose of 1×10^{10} VP/mouse for 8 hours. (C) Western blot of whole cell lysates from liver tissue of GSDMD^{-/-} mice treated with Ad-GFP-caspase-1-p10 or p20 alone or together at a dose of 1×10^{10} VP/mouse for indicated period of time showing expression of GFP, GSDMD, N-GSDMD, caspase-3 (C3), cleaved caspase-3 (Cl-C3), GSDME, and N-GSDME levels from liver tissue of GSDMD knockout mice. (D) Plasma ALT levels, TMR-red positive cells, and Western blot showing expression of GFP, GSDMD, and N-GSDMD in whole cell liver lysates of GSDMD^{-/-} mice treated with Ad-GSDMD for 24 hours and then with/without caspase-11 (C11)-p10 + p20 for 8 hours at a dose of 1×10^{10} VP/mouse. Immunofluorescent images in similar groups of mice showing TMR, red; Hoescht nuclear stain, blue; actin, green. Arrow = TMR-positive nuclei. Original magnification, $\times 40$. Data represent mean \pm SD. */#P < .05, **/##P < .01, ****P < .0001 vs respective Ctrl group unless specified; n = 5 mice/group. Images are representative across individual mice.



tissue samples were stored submerged in glutaraldehyde. For hepatocyte monolayer transmission electron microscopy, cells were washed twice with PBS, followed by PBS removal and addition of 1.5 mL 2.5% glutaraldehyde per well. Samples were stored in glutaraldehyde at 4°C in parafilm sealed 6-well plates. Samples were imaged at the CBI as described previously.⁵¹

Living Cell Image With IncuCyte Live-Cell Analysis System

Primary hepatocytes were plated in 12-well plates at a density of 2×10^5 cells/well. Medium was changed every other day, and treatments or controls were added as described in text to appropriate wells. Treated cells were imaged by IncuCyte Live-Cell Analysis System for 24 hours with imaging at $\times 20$ magnification. All 12 treatments were imaged in 4 unique fields per treatment every 30 minutes using a nuclear stain (IncuCyte NuLight Rapid Red; Sartorius, Essen Bioscience, Ann Arbor, MI), caspase-GFP-labeled constructs, cell death marker Annexin V (Annexin V NIR; Sartorius), phase contrast, and green (400 ms exposure) channels in IncuCyteS3 (Sartorius) platform, housed at 37°C with 5% CO₂.

Western Blot

Samples were lysed in lysis buffer with protease inhibitors and centrifuged at 16,100g for 10 minutes, and supernatant was collected. Protein concentration of supernatants was determined by BCA protein assay kit (Thermo Fisher Scientific). Denatured proteins were separated by sodium dodecyl sulfate–polyacrylamide gel electrophoresis and then transferred onto a polyvinylidene difluoride membrane at a current of 250 mA for 2 hours. Membrane was blocked in 5% milk for 1 hour at room temperature and then incubated overnight with primary antibody in 1% milk at 4°C. Membranes were washed 3 times \times 10 minutes in Tris-buffered saline with Tween-20 (TBS-T), incubated with horseradish peroxidase–conjugated secondary antibody for 1 hour at room temperature, and then washed 3 times \times 10 minutes in TBS-T before being developed for chemiluminescence.

Western images were quantified by densitometry using ImageJ software.

Real-Time Polymerase Chain Reaction

Total RNA was extracted using RNeasy Mini Kit (Qiagen, Hilden, Germany) according to manufacturer's instructions. From 1 μ g of RNA together with Reverse Transcription Supermix (Bio-Rad Laboratories, Hercules, CA), cDNA was generated and applied for real-time polymerase chain reaction (RT-PCR) analysis. Universal SYBR Green Supermix (Bio-Rad) and primer pairs specific for caspase-1 (forward: 5'-CCTCAAGTTTTGCCCTTTA-3'; reverse: 5'-CCTTCTTAATGCCATCATCTT-3'), caspase-11 (forward: 5'-CCT GAA GAG TTC ACA AGG CTT-3'; reverse: 5'-CCT TTC GTG TAG GGC CAT TG-3'), GSDMD (forward: 5'-CATGGCCTCAATGTGCTTGC-3'; reverse: 5'-GGTGGCAGG-GACACAGAAC-3'), GSDME (forward: 5'-ACAGGATGAGGT-CAGCAACC-3'; reverse: 5'-CAATCGCTGCACGATGCCAA-3'), and glyceraldehyde 3-phosphate dehydrogenase (GAPDH) (forward: 5'-TGACCACCAACTGCTTAGC-3'; reverse: 5'-GGCATGGACTGTGGTCATGAG-3') were used to prepare the RT-PCR mixes. All samples were assayed in duplicate, and results were normalized by GAPDH abundance.

LDH Assay

Lytic cell death after treatment was measured by LDH released into the medium. Fifty μ L of supernatant was transferred to a 96-well plate, and LDH reaction was performed using Pierce LDH Cytotoxicity Assay Kit (Thermo Fisher Scientific) according to manufacturer's instructions and analyzed by spectrophotometer (Biotech).

Statistics

Results are shown as mean \pm standard deviation (SD) for all the data with Gaussian distribution from at least 3 independent experiments. Data were analyzed by GraphPad Prism 8.0.1 software (San Diego, CA). Comparison between 2 experimental groups was performed by two-tailed unpaired *t* test. *P* < .05 was considered significantly different.

Figure 8. (See previous page). Morphologic features of hepatocyte pyroptosis in liver tissue. (A) H&E, IHC for CD45, and immunofluorescent TMR-red staining in liver tissue of WT and GSDMD^{-/-} mice treated with Ad-GFP-caspase-11-p20 alone or together with p10 at a dose of 1×10^{10} VP/mouse for indicated time periods. Left image: low magnification (original magnification, $\times 20$) images with higher magnification (original magnification, $\times 60$) insets. *Dotted lines* in liver H&E indicate areas of necrosis. *Black arrows* in H&E images indicate condensed nucleus. *Arrows* in IHC sections indicate CD45+ cells; TMR, *red*; Hoescht nuclear stain, *blue*; actin, *green*. Quantification of CD45+ cells and TMR-red positive cells in graphs below. (B) Transmission electron microscopy images from liver tissue of WT mice treated by GFP-caspase-11-p10 alone or together with p20 at a dose of 1×10^{10} VP/mouse for 8 hours. *m*, mitochondria; *n*, nucleus; ER, rough endoplasmic reticulum; *c*, chromatin; *arrow*, nuclear membrane; *arrowhead*, vacuoles from fragmented endoplasmic reticulum beaded with ribosomes. Original magnification, $\times 5000$ (5k) or $\times 20,000$ (20k). (C) Bone marrow-derived macrophages (BMDM) were isolated from C57BL/6 mice legs (tibia and femur) and cultured for 7 days at 37°C in a humidified 5% CO₂ incubator. After 7 days, BMDMs were plated in 6-well culture plate at 1×10^6 cells/mL and incubated overnight. Then BMDM and primary mouse hepatocytes (HCs) were treated with 1000 ng/mL and 100 ng/mL LPS for 24 hours, respectively. Expression of NINJ1 was detected by immunoblot analysis using 30 μ g of cell lysate (upper). In each group, at least 3 independent samples from different mice were examined. Data represent mean \pm SD. *****P* < .0001; *n* = 5 mice/group. Images are representative across individual mice.

References

- Cookson BT, Brennan MA. Pro-inflammatory programmed cell death. *Trends Microbiol* 2001;9:113–114.
- Kayagaki N, Wong MT, Stowe IB, Ramani SR, Gonzalez LC, Akashi-Takamura S, Miyake K, Zhang J, Lee WP, Muszynski A, Forsberg LS, Carlson RW, Dixit VM. Noncanonical inflammasome activation by intracellular LPS independent of TLR4. *Science* 2013;341:1246–1249.
- Hagar JA, Powell DA, Aachoui Y, Ernst RK, Miao EA. Cytoplasmic LPS activates caspase-11: implications in TLR4-independent endotoxic shock. *Science* 2013;341:1250–1253.
- Shi J, Zhao Y, Wang K, Shi X, Wang Y, Huang H, Zhuang Y, Cai T, Wang F, Shao F. Cleavage of GSDMD by inflammatory caspases determines pyroptotic cell death. *Nature* 2015;526:660–665.
- Kayagaki N, Stowe IB, Lee BL, O'Rourke K, Anderson K, Warming S, Cuellar T, Haley B, Roose-Girma M, Phung QT, Liu PS, Lill JR, Li H, Wu J, Kummerfeld S, Zhang J, Lee WP, Snipas SJ, Salvesen GS, Morris LX, Fitzgerald L, Zhang Y, Bertram EM, Goodnow CC, Dixit VM. Caspase-11 cleaves gasdermin D for non-canonical inflammasome signalling. *Nature* 2015;526:666–671.
- Broz P, Pelegrin P, Shao F. The gasdermins, a protein family executing cell death and inflammation. *Nat Rev Immunol* 2020;20:143–157.
- Wang Y, Gao W, Shi X, Ding J, Liu W, He H, Wang K, Shao F. Chemotherapy drugs induce pyroptosis through caspase-3 cleavage of a gasdermin. *Nature* 2017;547:99–103.
- Kambara H, Liu F, Zhang X, Liu P, Bajrami B, Teng Y, Zhao L, Zhou S, Yu H, Zhou W, Silberstein LE, Cheng T, Han M, Xu Y, Luo HR. Gasdermin D exerts anti-inflammatory effects by promoting neutrophil death. *Cell Rep* 2018;22:2924–2936.
- Zhang Z, Zhang Y, Xia S, Kong Q, Li S, Liu X, Junqueira C, Meza-Sosa KF, Mok TMY, Ansara J, Sengupta S, Yao Y, Wu H, Lieberman J. Gasdermin E suppresses tumour growth by activating anti-tumour immunity. *Nature* 2020;579:415–420.
- Zhou Z, He H, Wang K, Shi X, Wang Y, Su Y, Wang Y, Li D, Liu W, Zhang Y, Shen L, Han W, Shen L, Ding J, Shao F. Granzyme A from cytotoxic lymphocytes cleaves GSDMB to trigger pyroptosis in target cells. *Science* 2020:368.
- Wang Y, Liu Y, Liu Q, Zheng Q, Dong X, Liu X, Gao W, Bai X, Li Z. Caspase-1-dependent pyroptosis of peripheral blood mononuclear cells is associated with the severity and mortality of septic patients. *Biomed Res Int* 2020;2020:9152140.
- Bortolotti P, Faure E, Kipnis E. Inflammasomes in tissue damages and immune disorders after trauma. *Front Immunol* 2018;9:1900.
- Deng M, Tang Y, Li W, Wang X, Zhang R, Zhang X, Zhao X, Liu J, Tang C, Liu Z, Huang Y, Peng H, Xiao L, Tang D, Scott MJ, Wang Q, Liu J, Xiao X, Watkins S, Li J, Yang H, Wang H, Chen F, Tracey KJ, Billiar TR, Lu B. The endotoxin delivery protein HMGB1 mediates caspase-11-dependent lethality in sepsis. *Immunity* 2018;49:740–753 e7.
- Liu J, Du S, Kong Q, Zhang X, Jiang S, Cao X, Li Y, Li C, Chen H, Ding Z, Liu L. HSPA12A attenuates lipopolysaccharide-induced liver injury through inhibiting caspase-11-mediated hepatocyte pyroptosis via PGC-1 α -dependent acyl-CoA oxidase expression. *Cell Death Differ* 2020;27:2651–2667.
- Heo MJ, Kim TH, You JS, Blaya D, Sancho-Bru P, Kim SG. Alcohol dysregulates miR-148a in hepatocytes through FoxO1, facilitating pyroptosis via TXNIP overexpression. *Gut* 2019;68:708–720.
- Geng Y, Ma Q, Liu YN, Peng N, Yuan FF, Li XG, Li M, Wu YS, Li BL, Song WB, Zhu W, Xu WW, Fan J, Su L. Heatstroke induces liver injury via IL-1 β and HMGB1-induced pyroptosis. *J Hepatol* 2015;63:622–633.
- Gaul S, Leszczynska A, Alegre F, Kaufmann B, Johnson CD, Adams LA, Wree A, Damm G, Seehofer D, Calvente CJ, Povero D, Kisseleva T, Eguchi A, McGeough MD, Hoffman HM, Pelegrin P, Laufs U, Feldstein AE. Hepatocyte pyroptosis and release of inflammasome particles induce stellate cell activation and liver fibrosis. *J Hepatol* 2020;74:156–167.
- Sun Q, Gao W, Loughran P, Shapiro R, Fan J, Billiar TR, Scott MJ. Caspase 1 activation is protective against hepatocyte cell death by up-regulating beclin 1 protein and mitochondrial autophagy in the setting of redox stress. *J Biol Chem* 2013;288:15947–15958.
- Menzel CL, Sun Q, Loughran PA, Pape HC, Billiar TR, Scott MJ. Caspase-1 is hepatoprotective during trauma and hemorrhagic shock by reducing liver injury and inflammation. *Mol Med* 2011;17:1031–1038.
- Csak T, Ganz M, Pespisa J, Kodys K, Dolganiuc A, Szabo G. Fatty acid and endotoxin activate inflammasomes in mouse hepatocytes that release danger signals to stimulate immune cells. *Hepatology* 2011;54:133–144.
- Li W, Deng M, Loughran PA, Yang M, Lin M, Yang C, Gao W, Jin S, Li S, Cai J, Lu B, Billiar TR, Scott MJ. LPS induces active HMGB1 release from hepatocytes into exosomes through the coordinated activities of TLR4 and caspase-11/GSDMD signaling. *Front Immunol* 2020;11:229.
- Galluzzi L, Vitale I, Aaronson SA, Abrams JM, Adam D, Agostinis P, Alnemri ES, Altucci L, Amelio I, Andrews DW, Annicchiarico-Petruzzelli M, Antonov AV, Arama E, Baehrecke EH, Barlev NA, Bazan NG, Bernassola F, Bertrand MJM, Bianchi K, Blagosklonny MV, Blomgren K, Borner C, Boya P, Brenner C, Campanella M, Candi E, Carmona-Gutierrez D, Cecconi F, Chan FK, Chandel NS, Cheng EH, Chipuk JE, Cidlowski JA, Ciechanover A, Cohen GM, Conrad M, Cubillos-Ruiz JR, Czabotar PE, D'Angiolella V, Dawson TM, Dawson VL, De Laurenzi V, De Maria R, Debatin KM, DeBerardinis RJ, Deshmukh M, Di Daniele N, Di Virgilio F, Dixit VM, Dixon SJ, Duckett CS, Dynlacht BD, El-Deiry WS, Elrod JW, Fimia GM, Fulda S, Garcia-Saez AJ, Garg AD, Garrido C, Gavathiotis E, Golstein P, Gottlieb E, Green DR, Greene LA, Gronemeyer H, Gross A, Hajnoczky G, Hardwick JM, Harris IS, Hengartner MO, Hetz C, Ichijo H,

- Jaattela M, Joseph B, Jost PJ, Juin PP, Kaiser WJ, Karin M, Kaufmann T, Kepp O, Kimchi A, Kitsis RN, Klionsky DJ, Knight RA, Kumar S, Lee SW, Lemasters JJ, Levine B, Linkermann A, Lipton SA, Lockshin RA, Lopez-Otin C, Lowe SW, Luedde T, Lugli E, MacFarlane M, Madeo F, Malewicz M, Malorni W, Manic G, Marine JC, Martin SJ, Martinou JC, Medema JP, Mehlen P, Meier P, Melino S, Miao EA, Molkenkin JD, Moll UM, Munoz-Pinedo C, Nagata S, Nunez G, Oberst A, Oren M, Overholtzer M, Pagano M, Panaretakis T, Pasparakis M, Penninger JM, Pereira DM, Pervaiz S, Peter ME, Piacentini M, Pinton P, Prehn JHM, Puthalakath H, Rabinovich GA, Rehm M, Rizzuto R, Rodrigues CMP, Rubinsztein DC, Rudel T, Ryan KM, Sayan E, Scorrano L, Shao F, Shi Y, Silke J, Simon HU, Sistigu A, Stockwell BR, Strasser A, Szabadkai G, Tait SWG, Tang D, Tavernarakis N, Thorburn A, Tsujimoto Y, Turk B, Vanden Berghe T, Vandenabeele P, Vander Heiden MG, Villunger A, Virgin HW, Vousden KH, Vucic D, Wagner EF, Walczak H, Wallach D, Wang Y, Wells JA, Wood W, Yuan J, Zakeri Z, Zhivotovsky B, Zitvogel L, Melino G, Kroemer G. Molecular mechanisms of cell death: recommendations of the Nomenclature Committee on Cell Death 2018. *Cell Death Differ* 2018; 25:486–541.
23. Katsnelson MA, Rucker LG, Russo HM, Dubyak GR. K⁺ efflux agonists induce NLRP3 inflammasome activation independently of Ca²⁺ signaling. *J Immunol* 2015; 194:3937–3952.
24. Ruhl S, Shkarina K, Demarco B, Heilig R, Santos JC, Broz P. ESCRT-dependent membrane repair negatively regulates pyroptosis downstream of GSDMD activation. *Science* 2018;362:956–960.
25. Kaner RJ, Worgall S, Leopold PL, Stolze E, Milano E, Hidaka C, Ramalingam R, Hackett NR, Singh R, Bergelson J, Finberg R, Falck-Pedersen E, Crystal RG. Modification of the genetic program of human alveolar macrophages by adenovirus vectors in vitro is feasible but inefficient, limited in part by the low level of expression of the coxsackie/adenovirus receptor. *Am J Respir Cell Mol Biol* 1999;20:361–370.
26. Chen YL, Xu G, Liang X, Wei J, Luo J, Chen GN, Yan XD, Wen XP, Zhong M, Lv X. Inhibition of hepatic cells pyroptosis attenuates CLP-induced acute liver injury. *American Journal of Translational Research* 2016; 8:5685–5695.
27. Lebeauapin C, Proics E, de Bieville CH, Rousseau D, Bonnafous S, Patouraux S, Adam G, Lavallard VJ, Rovere C, Le Thuc O, Saint-Paul MC, Anty R, Schneck AS, Iannelli A, Gugenheim J, Tran A, Gual P, Bailly-Maitre B. ER stress induces NLRP3 inflammasome activation and hepatocyte death. *Cell Death Dis* 2015;6: e1879.
28. Wree A, Eguchi A, McGeough MD, Pena CA, Johnson CD, Canbay A, Hoffman HM, Feldstein AE. NLRP3 inflammasome activation results in hepatocyte pyroptosis, liver inflammation, and fibrosis in mice. *Hepatology* 2014;59:898–910.
29. Zhao H, Huang H, Alam A, Chen Q, Suen KC, Cui J, Sun Q, Ologunde R, Zhang W, Lian Q, Ma D. VEGF mitigates histone-induced pyroptosis in the remote liver injury associated with renal allograft ischemia-reperfusion injury in rats. *Am J Transplant* 2018; 18:1890–1903.
30. Zhang X, Luan J, Chen W, Fan J, Nan Y, Wang Y, Liang Y, Meng G, Ju D. Mesoporous silica nanoparticles induced hepatotoxicity via NLRP3 inflammasome activation and caspase-1-dependent pyroptosis. *Nanoscale* 2018;10:9141–9152.
31. Qiu T, Pei P, Yao X, Jiang L, Wei S, Wang Z, Bai J, Yang G, Gao N, Yang L, Qi S, Yan R, Liu X, Sun X. Taurine attenuates arsenic-induced pyroptosis and nonalcoholic steatohepatitis by inhibiting the autophagic-inflammasomal pathway. *Cell Death Dis* 2018;9:946.
32. Luan J, Zhang X, Wang S, Li Y, Fan J, Chen W, Zai W, Wang S, Wang Y, Chen M, Meng G, Ju D. NOD-like receptor protein 3 inflammasome-dependent IL-1 β accelerated ConA-induced hepatitis. *Front Immunol* 2018;9:758.
33. Lu Y, Xu S, Chen H, He M, Deng Y, Cao Z, Pi H, Chen C, Li M, Ma Q, Gao P, Ji Y, Zhang L, Yu Z, Zhou Z. CdSe/ZnS quantum dots induce hepatocyte pyroptosis and liver inflammation via NLRP3 inflammasome activation. *Biomaterials* 2016;90:27–39.
34. Ezquerro S, Mocha F, Fruhbeck G, Guzman-Ruiz R, Valenti V, Mugueta C, Becerril S, Catalan V, Gomez-Ambrosi J, Silva C, Salvador J, Colina I, Malagon MM, Rodriguez A. Ghrelin reduces TNF- α -induced human hepatocyte apoptosis, autophagy, and pyroptosis: role in obesity-associated NAFLD. *J Clin Endocrinol Metab* 2019;104:21–37.
35. Shi C, Wang Q, Rao Z, Shi Y, Wei S, Wang H, Lu X, Wang P, Lu L, Zhou H, Cheng F. Diabetes induces hepatocyte pyroptosis by promoting oxidative stress-mediated NLRP3 inflammasome activation during liver ischaemia and reperfusion injury. *Ann Transl Med* 2020; 8:739.
36. Eguchi A, Wree A, Feldstein AE. Biomarkers of liver cell death. *J Hepatol* 2014;60:1063–1074.
37. Kai J, Yang X, Wang Z, Wang F, Jia Y, Wang S, Tan S, Chen A, Shao J, Zhang F, Zhang Z, Zheng S. Oroxylin A promotes PGC-1 α /Mfn2 signaling to attenuate hepatocyte pyroptosis via blocking mitochondrial ROS in alcoholic liver disease. *Free Radic Biol Med* 2020; 153:89–102.
38. Zhong H, Liu M, Ji Y, Ma M, Chen K, Liang T, Liu C. Genipin reverses HFD-induced liver damage and inhibits UCP2-mediated pyroptosis in mice. *Cell Physiol Biochem* 2018;49:1885–1897.
39. Sun W, Zeng C, Liu S, Fu J, Hu L, Shi Z, Yue D, Ren Z, Zhong Z, Zuo Z, Cao S, Peng G, Deng J, Hu Y. Ageratina adenophora induces mice hepatotoxicity via ROS-NLRP3-mediated pyroptosis. *Sci Rep* 2018; 8:16032.
40. Khanova E, Wu R, Wang W, Yan R, Chen Y, French SW, Llorente C, Pan SQ, Yang Q, Li Y, Lazaro R, Ansong C, Smith RD, Bataller R, Morgan T, Schnabl B, Tsukamoto H. Pyroptosis by caspase11/4-gasdermin-D pathway in alcoholic hepatitis in mice and patients. *Hepatology* 2018;67:1737–1753.

41. Ambade A, Lowe P, Kodys K, Catalano D, Gyongyosi B, Cho Y, Iracheta-Vellve A, Adejumo A, Saha B, Calenda C, Mehta J, Lefebvre E, Vig P, Szabo G. Pharmacological inhibition of CCR2/5 signaling prevents and reverses alcohol-induced liver damage, steatosis, and inflammation in mice. *Hepatology* 2019;69:1105–1121.
42. Koh EH, Yoon JE, Ko MS, Leem J, Yun JY, Hong CH, Cho YK, Lee SE, Jang JE, Baek JY, Yoo HJ, Kim SJ, Sung CO, Lim JS, Jeong WI, Back SH, Baek IJ, Torres S, Solsona-Vilarrasa E, Rosa LC, Garcia-Ruiz C, Feldstein AE, Fernandez-Checa JC, Lee KU. Sphingomyelin synthase 1 mediates hepatocyte pyroptosis to trigger non-alcoholic steatohepatitis. *Gut* 2020.
43. Zhang LY, Zhan DL, Chen YY, Wang WH, He CY, Lin Y, Lin YC, Lin ZN. Aflatoxin B1 enhances pyroptosis of hepatocytes and activation of Kupffer cells to promote liver inflammatory injury via dephosphorylation of cyclooxygenase-2: an in vitro, ex vivo and in vivo study. *Arch Toxicol* 2019;93:3305–3320.
44. Sun Q, Scott MJ. Caspase-1 as a multifunctional inflammatory mediator: noncytokine maturation roles. *J Leukoc Biol* 2016;100:961–967.
45. Kayagaki N, Komfeld OS, Lee BL, Stowe IB, O'Rourke K, Li Q, Sandoval W, Yan D, Kang J, Xu M, Zhang J, Lee WP, McKenzie BS, Ulas G, Payandeh J, Roose-Girma M, Modrusan Z, Reja R, Sagolla M, Webster JD, Cho V, Andrews TD, Morris LX, Miosge LA, Goodnow CC, Bertram EM, Dixit VM. NINJ1 mediates plasma membrane rupture during lytic cell death. *Nature* 2021;591:131–136.
46. Hardy S, Kitamura M, Harris-Stansil T, Dai Y, Phipps ML. Construction of adenovirus vectors through Cre-lox recombination. *J Virol* 1997;71:1842–1849.
47. Li J, Chen Z, Stang MT, Gao W. Transiently expressed ATG16L1 inhibits autophagosome biogenesis and aberrantly targets RAB11-positive recycling endosomes. *Autophagy* 2017;13:345–358.
48. Yi Z, Deng M, Scott MJ, Fu G, Loughran PA, Lei Z, Li S, Sun P, Yang C, Li W, Xu H, Huang F, Billiar TR. IRG1/itaconate activates Nrf2 in hepatocytes to protect against liver ischemia-reperfusion injury. *Hepatology* 2020.
49. Lei Z, Deng M, Yi Z, Sun Q, Shapiro RA, Xu H, Li T, Loughran PA, Griepentrog JE, Huang H, Scott MJ, Huang F, Billiar TR. cGAS-mediated autophagy protects the liver from ischemia-reperfusion injury independently of STING. *Am J Physiol Gastrointest Liver Physiol* 2018; 314:G655–G667.
50. Ramos-Vara JA. Principles and methods of immunohistochemistry. *Methods Mol Biol* 2017;1641:115–128.
51. Sachdev U, Ferrari R, Cui X, Pius A, Sahu A, Reynolds M, Liao H, Sun P, Shinde S, Ambrosio F, Shiva S, Loughran P, Scott M. Caspase1/11 signaling affects muscle regeneration and recovery following ischemia, and can be modulated by chloroquine. *Mol Med* 2020; 26:69.

Received August 11, 2021. Accepted November 30, 2021.

Correspondence

Address correspondence to: Melanie J. Scott, MD, PhD, Department of Surgery Labs, University of Pittsburgh, NW653 MUH, 3459 Fifth Avenue, Pittsburgh, Pennsylvania 15213. e-mail: scottm@upmc.edu; fax: (412) 647-5959.

Acknowledgments

The authors thank Zachary Secunda and Danielle Reiser for technical assistance.

CRedit Authorship Contributions

Ping Sun (Conceptualization: Equal; Data curation: Lead; Formal analysis: Lead; Investigation: Lead; Project administration: Lead; Writing – original draft: Lead)

Zhongjie Yi (Formal analysis: Supporting; Investigation: Supporting)
 Hong Liao, MD (Data curation: Supporting; Formal analysis: Supporting)
 Patricia Loughran (Data curation: Supporting; Formal analysis: Supporting; Visualization: Equal)

Joud Mulla, MS (Data curation: Supporting; Methodology: Supporting)
 Guang Fu (Data curation: Supporting; Formal analysis: Supporting)
 Da Tang (Data curation: Supporting; Formal analysis: Supporting)
 Jie Fan, PhD (Conceptualization: Supporting; Funding acquisition: Supporting)

Timothy Billiar, MD (Conceptualization: Supporting; Methodology: Supporting; Project administration: Supporting)

Wentao Gao, PhD (Conceptualization: Supporting; Formal analysis: Supporting; Methodology: Supporting; Visualization: Supporting)

Melanie Scott (Conceptualization: Lead; Funding acquisition: Lead; Investigation: Lead; Project administration: Lead; Resources: Lead; Writing – review & editing: Lead)

Conflicts of interest

The authors disclose no conflicts.

Funding

Supported by the National Institutes of Health (NIH NIGMS R01GM102146 to MJS; NIH R01-HL-139547 to JF), VA Merit Award 1I01BX004838 to JF, VA BLR&D Award 1IK6BX004211 to JF, and National Science Foundation of China (No. 82002032 to PS). This work was also supported through the Pittsburgh Liver Research Center via support from NIH/NIDDK P30DK120531.